

# Non-Abelian Self-Correcting Quantum Memory

Po-Shen Hsin,<sup>1,2,\*</sup> Ryohei Kobayashi,<sup>3,4,†</sup> and Guanyu Zhu<sup>5,‡</sup>

<sup>1</sup>*Mani L. Bhaumik Institute for Theoretical Physics,  
475 Portola Plaza, Los Angeles, CA 90095, USA*

<sup>2</sup>*Department of Mathematics, King's College London, Strand, London WC2R 2LS, UK*

<sup>3</sup>*Department of Physics, Condensed Matter Theory Center, and Joint Quantum Institute,  
University of Maryland, College Park, Maryland 20742, USA*

<sup>4</sup>*School of Natural Sciences, Institute for Advanced Study, Princeton, NJ 08540, USA*

<sup>5</sup>*IBM Quantum, IBM T.J. Watson Research Center, Yorktown Heights, NY 10598 USA*

We construct a family of infinitely many new candidate non-Abelian self-correcting topological quantum memories in  $D \geq 5 + 1$  spacetime dimensions without particle excitations using local commuting non-Pauli stabilizer lattice models and field theories of  $\mathbb{Z}_2^3$  higher-form gauge fields with nontrivial topological action. We call such non-Pauli stabilizer models magic stabilizer codes. The family of topological orders have Abelian electric excitations and non-Abelian magnetic excitations that obey Ising-like fusion rules and non-Abelian braiding, including Borromean ring type braiding which is a signature of non-Abelian topological order, generalizing the dihedral group  $\mathbb{D}_8$  gauge theory in  $(2+1)D$ . The simplest example includes a new non-Abelian self-correcting memory in  $(5+1)D$  with Abelian loop excitations and non-Abelian membrane excitations. We prove the self-correction property and the thermal stability, and devise a probabilistic local cellular-automaton decoder.

## CONTENTS

I. Introduction	2	V. Cubic Theory in $(5+1)D$ as Non-Abelian TQFT	11
A. The model: non-Abelian cubic theory	3	A. TQFT Hilbert space	11
B. Review of quantum memory at finite temperature for loop toric code	4	B. Operators	11
II. Non-Pauli Stabilizer Model for Non-Abelian Cubic Theory	4	C. Non-Abelian braiding of magnetic operators	11
A. SPT Hamiltonian	4	1. Two-membrane braiding gives 0	11
B. Cubic theory Hamiltonian	6	D. “Borromean rings” braiding of membranes	12
1. Commuting non-Pauli stabilizer lattice model	6	VI. Cubic Theory from Compactifying Generalized Color Code	12
III. Non-Pauli Stabilizer Model for Cubic Theory in $(5+1)D$ : Loops and Membranes	7	VII. Self-Correcting Quantum Memory	13
A. Commuting non-Pauli stabilizer lattice Hamiltonian model	7	A. Interaction between system and environment	13
B. Ground states	8	1. Pauli noise model	14
C. Extended operators on the lattice	8	2. Stability against small excitations	15
1. Wilson surface operators	8	B. Self-correcting quantum memory with loops and membranes	15
2. Magnetic volume operators	8	C. Readout of the memory and decoding the logical information	17
D. Code distance	9	D. Generalization: general cubic theory without particles	17
IV. Cubic Theory in General Dimension as Non-Abelian TQFT	9	VIII. Discussion and Outlook	17
A. Field Theory	9	Acknowledgements	18
B. Hilbert space of TQFT	9	A. Obstruction to Non-Abelian Fusion	18
C. Operators	9	B. Review of Cup Product on Triangulated and Hypercubic Lattices	18
D. Cubic theories without particles	10	C. Logical CZ, S, Hadamard Gates in 4D Loop Toric Code	19
		1. Hadamard gate	19
		2. CZ and S gates	19

\* po-shen.hsin@kcl.ac.uk

† ryok@ias.edu

‡ guanyu.zhu@ibm.com

## I. INTRODUCTION

Self-correcting quantum memories are highly desirable for fault-tolerant quantum computing due to its passive protection at the hardware level and the connection to a local cellular automaton decoder [1, 2], as well as single-shot error correction [3]. All previous known examples of self-correction are essentially toric codes in four spatial dimensions or higher [1, 4, 5], which are Abelian topological order and belong to the class of Pauli stabilizer models. Recently, such (4+1)D models (space-time dimensions) have also been realized experimentally on the ion-trap platform and shows decoding advantage over (2+1)D surface codes [6]<sup>1</sup>. However, these self-correcting models are quite limited in terms of the computation power. For example, (4+1)D loop toric code can only realize logical Clifford gates, which hence cannot be universal. In order to get non-Clifford gates, one has to use (6+1)D toric codes or color codes proposed by Bombin et al [5], which requires a space overhead  $N = O(kd^3)$ , where  $N$  and  $k$  represent the number of physical and logical qubits while  $d$  is the code distance. On the other hand, since (2+1)D non-Abelian topological order such as Fibonacci string-net model has exhibited a universal logical gate set [24–28], a natural question is whether there exists a non-Abelian self-correcting memory at lower dimension which can potentially have higher computational power.

From the perspective of quantum phases of matter, a fundamental question is that whether topological orders can exist at finite temperature. It is known that (2+1)D toric code is unstable at finite temperature [2, 29–32] while the (4+1)D loop toric code is stable [1, 4, 5]. However, no examples beyond Abelian topological order or stabilizer models were known before this paper. This is because to find such non-Abelian self-correcting memory, one needs to have a topological order without particle excitations, which is quite challenging in the case of non-Abelian models. In fact, a no-go theorem was shown for non-Abelian topological order without particle excitations in (4+1)D [33–35]. Moreover, the usual (1-form) non-Abelian discrete gauge theory (i.e., quantum double models) [36] will necessarily have particle-like excitations.

Our present work solves this issue by turning to the higher-form gauge theory and in five or higher spatial dimensions. In particular, we have developed a new type of topological quantum field theory (TQFT) based on a

twisted version of  $\mathbb{Z}_2^3$  higher-form gauge theory. We further constructed the corresponding lattice models with non-Pauli (Clifford) stabilizers. We dub such a model a *magic stabilizer code* since it goes beyond the Pauli stabilizer formalism. We then prove that such non-Abelian models are indeed self-correcting, i.e., with an exponentially long memory time as system size grows, and hence is also thermally stable at finite temperature. We have also developed a local cellular-automaton decoder for such models. In particular, the simplest non-Abelian self-correcting quantum memories we discover in five spatial dimensions can potentially allow a universal quantum computing scheme with lower space overhead than the (6+1)D color code scheme. Interestingly, we find that our (5+1)D non-Abelian self-correcting memory can also be obtained from a twisted compactification of the (6+1)D color code in Ref. [5] down to five spatial dimensions. We also generalize the (5+1)D non-Abelian self-correcting memory to a family of infinitely many non-Abelian self-correcting memories above five spatial dimensions. The self-correcting quantum memories we discover have similar properties as the non-Abelian  $\mathbb{D}_8$  topological order observed in another experiment by Quantinuum [37]. Thus it is highly plausible that the new quantum memories can be realized by similar experiment setups on ion-trap platform using the long-range connection via movable ion qubits as in the recent experiment of (4+1)D loop toric code [6].

From the perspective of practical fault-tolerant quantum computation, a fundamental question is about the space-time overhead for the computation, including the overhead for both the quantum and classical operations in the computing process. In a typical case of an actively corrected quantum memory, one measures the error syndrome and then sends the syndrome information to the classical computer to decode it. The classical decoder then decides a recovery operation to correct the errors. These processes need non-local classical communications and the classical decoder requires computation time scaled with the system size. Since classical communication and gates are not infinitely faster than the quantum gates, such classical time overhead will make it impossible for the classical decoder to keep up with the advancing of quantum operations and to correct the errors timely when the system is large enough [2, 38]. Self-correcting memory is hence more desirable since it gets rid of the classical software and the associated time overhead and instead passively protects the quantum hardware from the errors. While such a passive protection might be challenging at the current stage from the engineering perspective, self-correcting memory is also useful even in the context of active error correction since it is always closely associated with an underlying local cellular-automaton decoder [1, 2]. Such a decoder is composed of local update rules at each time step and does not require non-local classical communication. It also does not have a decoding time overhead during the computation process except the final readout stage when the classical de-

<sup>1</sup> Higher dimensional topological orders above the physical dimension can be realized using long-range connections and are relevant for practical fault-tolerant quantum computation [7–9], and they are ubiquitous in quantum low-density parity-check (LDPC) codes [10–23].

coder no longer needs to catch up with the quantum operations. Although existing single-shot error correction schemes permit constant quantum time overhead [3], only self-correcting quantum memory can potentially achieve both constant quantum and classical time overhead. In fact, there exists a scheme for implementing universal logical gate set with constant-depth geometrically non-local circuits acting on a non-Abelian topological code [39–41] where the time overhead is expected to be  $O(d/\log d)$  ( $d$  is the code distance) due to the stretching of the support of error clusters by a constant factor. If such a scheme can be adapted to a non-Abelian self-correcting memory where the stretched error can be shrunk back in constant time, constant time overhead will be achieved for both the quantum and classical operations during the computation stage.

Recall that non-Abelian self-correcting quantum memories correspond to novel non-Abelian topological orders without particles. Nevertheless, non-Abelian topological orders above  $D = 4$  spacetime dimension are less understood except for topological orders with particles (see e.g. [42]), where the particles arise from the electric charges due to gauging an ordinary symmetry. On the other hand, topological orders without particles are highly constrained: the lowest-dimensional excitations must obey Abelian fusion rule (see e.g. [33–35]). For instance, if the lowest-dimensional nontrivial excitation is a membrane, then it must obey Abelian fusion rule. On the other hand, when there exist nontrivial loop excitations, the membrane excitations do not need to obey Abelian fusion, and they can be non-Abelian. Non-Abelian TQFTs without particles can only exist at or above spacetime dimension  $D \geq 5+1$ . To see this, we note that non-Abelian fusion of  $k$ -dimensional excitations with  $k \geq 1$  requires  $(k-1)$ -dimensional excitations in order to produce a consistent fusion rule after shrinking the  $k$ -dimensional excitations on a circle: without nontrivial  $(k-1)$ -dimensional excitations, shrinking on a circle would produce the inconsistent fusion  $1 \times 1 = 1 + 1 + \dots$  from the non-Abelian fusion of  $k$ -dimensional excitations (see e.g. [33–35] and appendix A). In addition, we require  $(k-1) \geq 1$  to avoid particles. Remote detectability, i.e. an  $n$ -dimensional excitation must have mutual braiding with some  $(D-n-3)$ -dimensional excitations in well-defined TQFTs [43–46], further implies that there are also  $(D-k-3)$ ,  $(D-k-2)$ -dimensional excitations.<sup>2</sup> Demanding them to be at least 1-dimensional gives  $k \leq (D-4)$ . Thus  $2 \leq k \leq (D-4)$ , and  $D \geq 6$ . We will provide explicit models for a family of infinite many new non-Abelian topological orders without particles at every  $D \geq 6$  spacetime dimensions.

<sup>2</sup> Similar to non-Abelian anyon theories, here we consider non-Abelian excitations that are not condensation defects [47]. Such condensation defects do not satisfy remote detectability. Without such requirement, the lowest spacetime dimension would be  $D = 5$ , e.g. the Cheshire membrane in  $(4+1)$ D loop toric code is non-Abelian, but it is a condensation of the Abelian loop excitation.

## A. The model: non-Abelian cubic theory

In this work we will construct a family of Non-Abelian self-correcting quantum memories. This is done by gauging the global symmetry of certain class of symmetry-protected topological (SPT) phases with higher-form symmetries in  $D \geq 5 + 1$  spacetime dimensions. This construction is regarded as a generalization of  $(2+1)$ D non-Abelian  $\mathbb{D}_8$  gauge theory, which is obtained by gauging the SPT phase with  $\mathbb{Z}_2^3$  symmetry.

We start with the SPT phase protected by  $\mathbb{Z}_2$   $(l-1)$ -form symmetry,  $(m-1)$ -form symmetry and  $(n-1)$ -form symmetry in  $D$  spacetime dimensions, with  $l+m+n = D$ . The response action for the SPT phase is given by

$$\pi \int A_l \cup B_m \cup C_n, \quad (1)$$

where  $A_l, B_m, C_n$  are the background gauge fields. In Appendix B we review the definition of cup product  $\cup$ .

After gauging the  $\mathbb{Z}_2^3$  symmetry of the above SPT phase, we obtain certain class of non-Abelian topological order. We will call them generalized  $\mathbb{D}_8$  theories or the cubic theories.<sup>3</sup> They are described by  $\mathbb{Z}_2$   $l$ -form,  $m$ -form and  $n$ -form gauge theories in  $D$  spacetime dimensions, with the topological action

$$\pi \int a_l \cup b_m \cup c_n, \quad (2)$$

where  $a_l, b_m, c_n$  are the respective dynamical gauge fields. The theory describes non-Abelian topological order: the fusion rules of the magnetic operators that create magnetic flux for  $a_l, b_m, c_n$  are non-invertible. For instance, fusing the  $(D-l-1)$ -dimensional magnetic membrane operator for the gauge field  $a_l$  gives

$$M^{(1)}(M_{D-l-1}) \times M^{(1)}(M_{D-l-1}) = \sum_{\gamma_m, \gamma'_n} W^{(2)}(\gamma_m) W^{(3)}(\gamma'_n), \quad (3)$$

where  $W^{(2)} = (-1)^{\int b_m}$  and  $W^{(3)} = (-1)^{\int c_n}$  are Wilson surface operators, and the sum is over  $\gamma_m \in H_m(M_{D-l-1})$ ,  $\gamma'_n \in H_n(M_{D-l-1})$ . The right hand side is a sum of simple objects, and thus the fusion is non-Abelian. When  $l = m = n = 1, D = 3$ , the above topological order gives a  $(2+1)$ D  $\mathbb{D}_8$  gauge theory [37, 48] with non-Abelian fusion rule of anyons (3). In addition, we also show that the magnetic excitations obey non-Abelian braiding, including Borromean ring type braiding of three different magnetic excitations given by a sign—which is a signature of non-Abelian topological order.

<sup>3</sup> Despite the naming similarity, the theories are not related to Haah’s cubic code.

For each member in the family, we construct commuting non-Pauli stabilizer lattice models on any triangulated spatial lattice, and in particular on hypercubic lattice. We call such non-Pauli stabilizer models magic stabilizer codes.

We will show that when  $l, m, n$  obey  $2 \leq l, m, n$ , the theory does not have particle excitations. Thus the models provide a family of infinitely many non-Abelian topological order without particles in  $D \geq 6$ , such as  $D = 6$  and  $l = m = n = 2$ , where the theory describes Abelian loop excitations and non-Abelian membrane excitations. We will argue that the theories provide thermally stable quantum memory.

### B. Review of quantum memory at finite temperature for loop toric code

Let us review the basic property of self-correcting quantum memory discussed in Ref. [1] for the example of loop-only  $\mathbb{Z}_2$  toric code in (4+1)D following a Peierls argument. The Hilbert space has physical qubit on each face of the 4d cubic lattice, and the stabilizer Hamiltonian is

$$H = H_{\text{Gauss}} + H_{\text{Flux}} = - \sum_e \prod_{f \in \partial f} X_f - \sum_c \prod_{f \in \partial c} Z_f. \quad (4)$$

The basic excitations are loop excitations created by membrane operators  $\prod X_f$  and  $\prod Z_f$ . Take the error given by electric loop excitation of length  $\ell$  measured in the lattice spacing, which violates  $\ell$  of the Gauss law terms in the Hamiltonian and have energy cost  $E(\ell) = 2\ell\epsilon_0$  where  $\epsilon_0$  is the energy unit of the Hamiltonian. There are  $n(\ell)$  such configuration of length  $\ell$ , and they are suppressed by the Boltzmann factor  $e^{-\beta E(\ell)}$ . Whether large errors are suppressed at low temperature depends on the competition of the this entropy effect and the Boltzmann suppression. The large loop excitation errors are suppressed when

$$e^{-\beta E(\ell)} n(\ell) \ll 1. \quad (5)$$

where  $\beta = 1/(k_B T)$  for temperature  $T$  and Boltzmann constant  $k_B$ . The multiplicity of loops of length  $\ell$  is

$$n(\ell) \sim \text{Polynomial}(\ell) \mu^\ell, \quad (6)$$

where  $\mu \sim 6.77$  is the connectivity on 4D hypercubic lattice [49], and only self-avoiding loops are counted by resolving the intersection points without loss of generality. At low temperature, the large loops are exponentially suppressed. The critical temperature below which the errors are suppressed is

$$T_c \sim (2/\log \mu) \epsilon_0 / k_B. \quad (7)$$

A more rigorous argument for the self-correcting property using the Lindbladian evolution under Pauli noise model is discussed in e.g. [50], and we will use the method

there to prove the self-correcting property of our non-Abelian quantum memory.

The work is organized as follows. In Section II we discuss a family of non-Pauli stabilizer codes with only loops and non-Abelian membrane excitations. In Section III we describe the fusion rules of the excitations in the (5+1)D lattice model. In Section IV we discuss a family of infinitely many non-Abelian TQFTs in any dimension dubbed a Cubic theory, which effectively describes our lattice model. In Section V, we describe the braiding involving non-Abelian excitations. In Section VI we see that the cubic theory is obtained from the compactification of the toric code in one higher dimension. In Section VII we argue that our model provides the self-correcting quantum memory at finite temperature. There are several appendices. In Appendix A we describe an obstruction to non-Abelian extended excitations in TQFTs. In Appendix B we summarized some properties of cup product on triangulated or hypercubic lattices. In Appendix C we discuss the CZ,S and Hadamard logical gates in 4D loop toric code.

## II. NON-PAULI STABILIZER MODEL FOR NON-ABELIAN CUBIC THEORY

Let us construct a local commuting non-Pauli stabilizer Hamiltonian for the Cubic theory in  $D = d+1$  spacetime dimensions. We can begin by constructing a Hamiltonian model for the SPT phase with  $\mathbb{Z}_2$   $(l-1)$ -form symmetry,  $(m-1)$ -form symmetry, and  $(n-1)$ -form symmetry with  $l+m+n = D$ , and then gauge these symmetries minimally.

### A. SPT Hamiltonian

We consider a hypercubic lattice in  $d$ -dimensional Euclidean space. We introduce a qubit on each  $(l-1)$ -dimensional hypercube,  $(m-1)$ -dimensional hypercube,  $(n-1)$ -dimensional hypercube, acted by Pauli operators  $\{\tilde{X}^i, \tilde{Y}^i, \tilde{Z}^i\}$  with  $1 \leq i \leq 3$  respectively. We use a tilde on the Pauli operators to distinguish them from the Pauli operators in the gauged model we will present later. Denote the  $\mathbb{Z}_2$  variables  $\lambda^i = (1 - \tilde{Z}^i)/2$ . In the basis of Pauli  $Z$  operators,  $\lambda^i$  is naturally regarded as  $\mathbb{Z}_2$   $j$ -cochains ( $j = l-1, m-1, n-1$ ) for  $i = 1, 2, 3$ , namely a function from the  $j$ -dimensional hypercubes to the  $\mathbb{Z}_2$  values  $\{0, 1\}$ .

Let us now describe the Hamiltonian for the SPT phase with the topological response action given by

$$\pi \int A_l \cup B_m \cup C_n, \quad (8)$$

with  $A_l, B_m, C_n$  the background gauge fields. This is a higher-form generalization of the group cohomology SPT phases discussed in [51], corresponding to the higher-form analogue of ‘‘type III cocycle’’ SPT phase [52, 53]. We



will follow similar method in [51] to construct the Hamiltonian. Other examples of lattice models for higher-form SPT phases constructed in this way are discussed in e.g. [54, 55].

The SPT Hamiltonian is most simply expressed by utilizing the operation of cochains called cup product, denoted by  $\cup$ . For more details, see e.g. [42, 56–59].

On hypercubic lattice, the cup product  $\alpha_i \cup \beta_j$  of  $\mathbb{Z}_2$   $i$ -cochain  $\alpha_i$  and  $j$ -cochain  $\beta_j$  produces a  $(i+j)$ -cochain, and its value on  $(i+j)$ -dimensional hypercube  $s_{i+j}$  that span the coordinates  $(x^1, x^2, \dots, x^{i+j}) \in [0, 1]^{i+j}$  is given by

$$\alpha_i \cup \beta_j(s_{i+j}) = \sum_I \alpha_i([0, 1]^I) \beta_j\left((x^I = 1, x^{\bar{I}} = 0) + [0, 1]^{\bar{I}}\right), \quad (9)$$

where the summation is over the different sets  $I$  of  $i$  coordinates out of the  $(i+j)$  coordinates  $x^1, \dots, x^{i+j}$ ,  $\bar{I}$  denotes the remaining  $j$  coordinates. In each term in the sum,  $\alpha_i, \beta_j$  are evaluated on an  $i$ -dimensional hypercube and an  $j$ -dimensional hypercube, where the two hypercubes share a single vertex ( $x^I = 1, x^{\bar{I}} = 0$ ):

- $[0, 1]^I$  is the  $i$ -dimensional unit hypercube starting from  $(x^I = 0, x^{\bar{I}} = 0)$  and ending at  $(x^I = 1, x^{\bar{I}} = 0)$ , i.e.  $[0, 1]^I = \{0 \leq x^\mu \leq 1, x^\nu = 0 : \mu \in I, \nu \in \bar{I}\}$ .
- $(x^I = 1, x^{\bar{I}} = 0) + [0, 1]^{\bar{I}}$  is the  $l$ -dimensional hypercube in the  $\bar{I}$  directions starting from  $(x^I = 1, x^{\bar{I}} = 0)$  and ending at  $(x^I = 1, x^{\bar{I}} = 1)$ , i.e.  $(x^I = 1, x^{\bar{I}} = 0) + [0, 1]^{\bar{I}} = \{x^\mu = 1, 0 \leq x^\nu \leq 1 : \mu \in I, \nu \in \bar{I}\}$ .

For instance, the sum in the cup product (9) for  $i = 1, j = 2$  is described in Figure 1. It sums over the possible sequence of two hypercubes sharing a single vertex, starting at  $(0, 0, \dots, 0)$  and ending at  $(1, 1, \dots, 1)$ .

Now we are ready to describe the SPT Hamiltonian. It is obtained by conjugating the trivial SPT Hamiltonian by an entangler. The trivial Hamiltonian is given by

$$H^0 = - \sum_{s_{l-1}} \tilde{X}_{s_{l-1}}^1 - \sum_{s_{m-1}} \tilde{X}_{s_{m-1}}^2 - \sum_{s_{n-1}} \tilde{X}_{s_{n-1}}^3 \quad (10)$$

where  $s_k$  are  $k$ -dimensional hypercubes. We then consider the entangler

$$U = (-1) \int \lambda_{l-1}^1 \cup d\lambda_{m-1}^2 \cup d\lambda_{n-1}^3, \quad (11)$$

where  $d$  is the coboundary of  $\mathbb{Z}_2$  cochains; for a given  $\mathbb{Z}_2$   $k$ -cochain  $\alpha$ ,  $d\alpha$  is a  $\mathbb{Z}_2$   $(k+1)$ -cochain defined as

$$d\alpha(s_{k+1}) = \sum_{s_k \in \partial s_{k+1}} \alpha(s_k). \quad (12)$$

Recall that  $\lambda^i$  is regarded as an operator-valued  $\mathbb{Z}_2$  cochains in the basis of Pauli  $Z$  operators, and then the

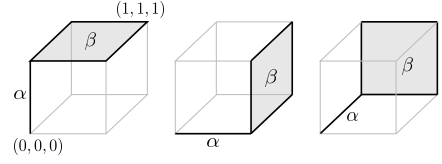


FIG. 1. The cup product  $\alpha_1 \cup \beta_2$  evaluated on a 3d cube. It sums over the possible sequence of a 1d edge and a 2d square sharing a single vertex, starting at  $(0, 0, 0)$  and ending at  $(1, 1, 1)$ .

cochain  $\lambda_{l-1}^1 \cup d\lambda_{m-1}^2 \cup d\lambda_{n-1}^3$  is a  $d$ -cochain. The integral in Eq. (11) is over  $d$ -chains in the whole space. One can re-express the operator-valued cochain as  $\lambda_k^i = \sum_{\tilde{s}_k} \hat{N}^i \tilde{s}_k$  in Eq. (11), where  $\hat{N}^i = (1 - \tilde{Z}^i)/2$  is the quantum operator and the classical variable  $\tilde{s}_k$  is a  $k$ -cochain that takes value 1 on a single hypercube  $s_k$  and zero otherwise. The above entangler in Eq. (11) can hence be re-written in terms of quantum gates as:

$$U = (-1) \int \hat{N}^1 \tilde{s}_{l-1} \cup \hat{N}^2 \tilde{d}\tilde{s}_{m-1} \cup \hat{N}^3 \tilde{d}\tilde{s}_{n-1} \\ = \prod_{\tilde{s}_{l-1}, \tilde{s}_{m-1}, \tilde{s}_{n-1}} \text{CCZ}_{1,2,3}^{\int \tilde{s}_{l-1} \cup d\tilde{s}_{m-1} \cup d\tilde{s}_{n-1}},$$

where we have used the gate identity  $(-1)^{\hat{N}^1 \hat{N}^2 \hat{N}^3} = \text{CCZ}_{1,2,3}$  since  $\text{CCZ}_{1,2,3} |N^1, N^2, N^3\rangle = (-1)^{N^1 N^2 N^3} |N^1, N^2, N^3\rangle$  ( $N^i \in \{0, 1\}$  is the eigenvalue of  $\hat{N}^i$ ). Note the exponent  $\int \tilde{s}_{l-1} \cup d\tilde{s}_{m-1} \cup d\tilde{s}_{n-1} \in \{0, 1\}$  is a classical  $\mathbb{Z}_2$  variable which determines whether the CCZ gate on qubits supported on hypercubes  $\tilde{s}_{l-1}, \tilde{s}_{m-1}$  and  $\tilde{s}_{n-1}$  is applied (value 1) or not (value 0).

The SPT Hamiltonian is given by  $H_{\text{SPT}}$  is obtained by  $H_{\text{SPT}} = UH^0U^\dagger$ ,

$$H_{\text{SPT}} = - \sum_{s_{l-1}} \tilde{X}_{s_{l-1}}^1 (-1) \int \tilde{s}_{l-1} \cup d\lambda_{m-1}^2 \cup d\lambda_{n-1}^3 \\ - \sum_{s_{m-1}} \tilde{X}_{s_{m-1}}^2 (-1) \int d\lambda_{l-1}^1 \cup \tilde{s}_{m-1} \cup d\lambda_{n-1}^3 \\ - \sum_{s_{n-1}} \tilde{X}_{s_{n-1}}^3 (-1) \int d\lambda_{l-1}^1 \cup d\lambda_{m-1}^2 \cup \tilde{s}_{n-1} \\ = - \sum_{s_{l-1}} \tilde{X}_{s_{l-1}}^1 \prod_{\tilde{s}_{m-1}, \tilde{s}_{n-1}} \text{CZ}_{2,3}^{\int \tilde{s}_{l-1} \cup d\tilde{s}_{m-1}^2 \cup d\tilde{s}_{n-1}^3} \\ - \sum_{s_{m-1}} \tilde{X}_{s_{m-1}}^2 \prod_{\tilde{s}_{l-1}, \tilde{s}_{n-1}} \text{CZ}_{1,3}^{\int d\tilde{s}_{l-1}^1 \cup \tilde{s}_{m-1} \cup d\tilde{s}_{n-1}^3} \\ - \sum_{s_{n-1}} \tilde{X}_{s_{n-1}}^3 \prod_{\tilde{s}_{l-1}, \tilde{s}_{m-1}} \text{CZ}_{1,2}^{\int d\tilde{s}_{l-1}^1 \cup d\tilde{s}_{m-1}^2 \cup \tilde{s}_{n-1}}, \quad (13)$$

where we have derived the second equality by rewriting the operator-valued cochain as  $\lambda_k^i = \sum_{\tilde{s}_k} \hat{N}^i \tilde{s}_k$  as before, and used the identity  $(-1)^{\hat{N}^i \hat{N}^j} = \text{CZ}_{i,j}$ . The exponent again determines the support of the CZ gates.

SPT	$\xrightarrow{\text{Gauge } \mathbb{Z}_2^3}$	Cubic theory
$\tilde{X}_{s_{l-1}}^1$	$\leftrightarrow$	$\prod_{s_{l-1} \subset \partial s_l} X_{s_l}^1$
$\prod_{s_{l-1} \subset \partial s_l} \tilde{Z}_{s_{l-1}}^1$	$\leftrightarrow$	$Z_{s_l}^1$
$d\lambda_{l-1}^1, d\lambda_{m-1}^2, d\lambda_{n-1}^3$	$\leftrightarrow$	$a_l, b_m, c_n$

TABLE I. The  $\mathbb{Z}_2^3$  gauging induces the above mapping between the Pauli operators and cochains. Similar relations also hold for  $\{X^2, Z^2\}, \{X^3, Z^3\}$ . See Fig. 2 for an illustration for  $l = 1$  on 2D square lattice.

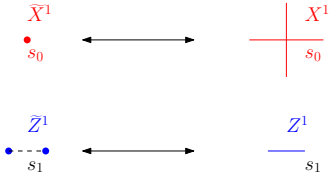


FIG. 2. Mapping of operators under the gauging operation in table I for  $l = 1$  on 2d square lattice. Here  $s_0$  and  $s_1$  represent the 0- and 1-dimensional hypercubes, i.e., a vertex and an edge respectively.

## B. Cubic theory Hamiltonian

We can gauge the symmetries of the SPT Hamiltonian  $H_{\text{SPT}}$  following the method in e.g. [48, 60–62] by introducing  $\mathbb{Z}_2$  gauge fields as qubits on each  $l, m, n$  hypercubes, acted by the Pauli operators  $X^i, Y^i, Z^i$  with  $i = 1, 2, 3$  for the three types of qubits.

Denote the  $\mathbb{Z}_2$  cochains  $a_l = (1 - Z^1)/2$ ,  $b_m = (1 - Z^2)/2$ ,  $c_n = (1 - Z^3)/2$ . After gauge fixing, one can suppress the original qubits  $\{\tilde{X}^i, \tilde{Y}^i, \tilde{Z}^i\}$ , and the gauged theory is defined on the Hilbert space of qubits for gauge fields  $\{X^i, Y^i, Z^i\}$ . In short, the  $\mathbb{Z}_2^3$  gauging is regarded as a duality map from the Hilbert space of  $\{\tilde{X}^i, \tilde{Y}^i, \tilde{Z}^i\}$  to that of  $\{X^i, Y^i, Z^i\}$  with the Pauli operators mapped as shown in Table I (see also Fig. 2 for an illustration).

The Hamiltonian of the gauged theory is then given by

$$\begin{aligned}
H_{\text{Cubic}} &= H_{\text{Gauss}} + H_{\text{Flux}}, \\
H_{\text{Gauss}} &= - \sum_{s_{l-1}} \left( \prod_{s_{l-1} \subset \partial s_l} X_{s_l}^1 \right) (-1)^{\int \tilde{s}_{l-1} \cup b_m \cup c_n} \\
&\quad - \sum_{s_{m-1}} \left( \prod_{s_{m-1} \subset \partial s_m} X_{s_m}^2 \right) (-1)^{\int a_l \cup \tilde{s}_{m-1} \cup c_n} \\
&\quad - \sum_{s_{n-1}} \left( \prod_{s_{n-1} \subset \partial s_n} X_{s_n}^3 \right) (-1)^{\int a_l \cup b_m \cup \tilde{s}_{n-1}} \\
&= - \sum_{s_{l-1}} \left( \prod_{s_{l-1} \subset \partial s_l} X_{s_l}^1 \right) \prod_{s'_m, s'_n} CZ_{2,3}^{\int \tilde{s}_{l-1} \cup \tilde{s}'_m \cup \tilde{s}'_n} \\
&\quad - \sum_{s_{m-1}} \left( \prod_{s_{m-1} \subset \partial s_m} X_{s_m}^2 \right) \prod_{s'_l, s'_n} CZ_{1,3}^{\int \tilde{s}'_l \cup \tilde{s}_{m-1} \cup \tilde{s}'_n} \\
&\quad - \sum_{s_{n-1}} \left( \prod_{s_{n-1} \subset \partial s_n} X_{s_n}^3 \right) \prod_{s'_l, s'_m} CZ_{1,2}^{\int \tilde{s}'_l \cup \tilde{s}'_m \cup \tilde{s}_{n-1}} \quad (14)
\end{aligned}$$

where  $s_j$  are  $j$ -dimensional hypercubes on the lattice, and there are only constant number of terms in each product. The flux terms  $H_{\text{flux}}$  are

$$\begin{aligned}
H_{\text{Flux}} &= - \sum_{s_{l+1}} \left( \prod_{s_l \subset \partial s_{l+1}} Z_{s_l}^1 \right) - \sum_{s_{m+1}} \left( \prod_{s_m \subset \partial s_{m+1}} Z_{s_m}^2 \right) \\
&\quad - \sum_{s_{n+1}} \left( \prod_{s_n \subset \partial s_{n+1}} Z_{s_n}^3 \right). \quad (15)
\end{aligned}$$

In the Gauss law Hamiltonian  $H_{\text{Gauss}}$ , the term involving cup product e.g.,  $(-1)^{\int \tilde{s}_{l-1} \cup b_m \cup c_n}$  is expressed as the product of  $CZ_{2,3}$  operators involving two qubits at the position of  $b_m, c_n$  in a similar manner as Eq. (13). In general, each term of  $H_{\text{Gauss}}$  consists of the product of  $X^i$  and  $CZ_{j,k}$  for distinct  $j, k \neq i$ .

### 1. Commuting non-Pauli stabilizer lattice model

We note that the Gauss law terms  $H_{\text{Gauss}}$  only commute among themselves on the zero flux sector. To make them exactly commute with each other, we can modify the Gauss law term by multiplying them with projectors to zero fluxes. We note that the flux projectors commute with each term in  $H_{\text{Gauss}}$ , and thus the ordering of the projectors do not matter. This gives commuting Gauss law Hamiltonian:

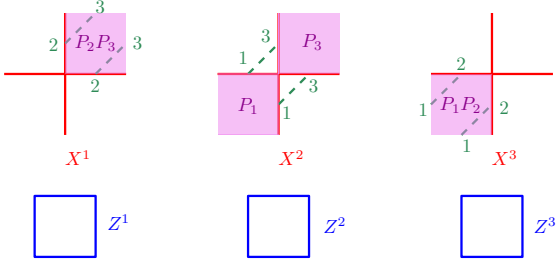


FIG. 3. Non-Pauli stabilizer model for  $D = 3, l = m = n = 1$  cubic theory, which is equivalent to ordinary  $\mathbb{D}_8$  gauge theory in (2+1)D. Here  $P_i(f) = \frac{1 + \prod_{e \in \partial f} Z_e^i}{2}$  is the projector to zero flux on face  $f$ . The dashed line with endpoints  $i, j$  is the operator  $CZ_{i,j}$  on the qubits  $i, j$  on the edges connected by the line. The upper figures can multiply with addition flux projectors and still maintain the commuting property.

$$\begin{aligned}
H'_{\text{Gauss}} = & - \sum_{s_{l-1}} \left( \prod_{s_{l-1} \subset \partial s_l} X_{s_l}^1 \right) (-1)^{\int \tilde{s}_{l-1} \cup b_m \cup c_n} \\
& \prod_{s'_{m-1}} \left( \frac{1 + (-1)^{\int \tilde{s}_{l-1} \cup \tilde{s}'_{m-1} \cup d c_n}}{2} \right) \prod_{s''_{n-1}} \left( \frac{1 + (-1)^{\int \tilde{s}_{l-1} \cup d b_m \cup \tilde{s}''_{n-1}}}{2} \right) \\
& - \sum_{s_{m-1}} \left( \prod_{s_{m-1} \subset \partial s_m} X_{s_m}^2 \right) (-1)^{\int a_l \cup \tilde{s}_{m-1} \cup c_n} \\
& \prod_{s'_{l-1}} \left( \frac{1 + (-1)^{\int \tilde{s}'_{l-1} \cup \tilde{s}_{m-1} \cup d c_n}}{2} \right) \prod_{s''_{n-1}} \left( \frac{1 + (-1)^{\int d a_l \cup \tilde{s}_{m-1} \cup \tilde{s}''_{n-1}}}{2} \right) \\
& - \sum_{s_{n-1}} \left( \prod_{s_{n-1} \subset \partial s_n} X_{s_n}^3 \right) (-1)^{\int a_l \cup b_m \cup \tilde{s}_{n-1}} \\
& \prod_{s'_{l-1}} \left( \frac{1 + (-1)^{\int \tilde{s}'_{l-1} \cup d b_m \cup \tilde{s}_{n-1}}}{2} \right) \prod_{s''_{m-1}} \left( \frac{1 + (-1)^{\int d a_l \cup \tilde{s}''_{m-1} \cup \tilde{s}_{n-1}}}{2} \right). \tag{16}
\end{aligned}$$

Here we list several important properties of the Cubic theory Hamiltonian:

*a. Locality of Hamiltonian* Each term in the Hamiltonian (16) is local. This is because on hypercubic lattice, for a given simplex  $s_j$  and integers  $k, k'$ ,  $\tilde{s}_j \cup \tilde{s}_k \neq 0$ ,  $\tilde{s}_{k'} \cup \tilde{s}_j \neq 0$  for finite number of simplices  $s_k, s_{k'}$  independent of the system size. More explicitly, the number of  $s_k$  is given by choosing  $k$  positive spatial directions in the complementary  $(D - j - 1)$  spatial directions, which is  $\binom{D - j - 1}{k}$ . Similarly, the number of  $s_{k'}$  is  $\binom{D - j - 1}{k'}$ . For example, if  $k = D - j - 1$  or  $k' = D - j - 1$ , there is a unique choice of  $s_k$  or  $s_{k'}$ .

*b. Local commuting non-Pauli stabilizer Hamiltonian*  
The modified Hamiltonian

$$H'_{\text{Cubic}} = H'_{\text{Gauss}} + H_{\text{Flux}} \tag{17}$$

is a sum of local commuting terms and has the same ground states as the Hamiltonian  $H_{\text{Cubic}}$ . We remark that the cup product expression allows us to define the model on any lattice that admits a triangulation. For example, when  $D = 3, l = m = n = 1$ , the model is illustrated in Figure 3. The lattice model defines a non-Pauli stabilizer code describing non-Abelian topological orders, and we will call it magic stabilizer code.

*c. Excitations* Since the Hamiltonian is a sum of local commuting terms, we can analyze the errors for each term independently, just as in the Calderbank-Shor-Steele (CSS) codes.

Since the Hamiltonian terms commute with each other, the excited states are eigenstates of the Hamiltonian terms. The Gauss law terms can have eigenvalues in  $\{-1, 0, 1\}$ , while the flux terms can have eigenvalues in  $\{-1, 1\}$ . There are electric and magnetic excitations, labelled by the eigenvalues of the Hamiltonian terms. The basic electric excitations are given by violations of the Gauss law term by  $1 - (-1) = 2$  but not the flux term. The basic magnetic excitations are given by violations of the flux terms by  $1 - (-1) = 2$  and violation of the Gauss law terms by  $0 - (-1) = 1$ .

### III. NON-PAULI STABILIZER MODEL FOR CUBIC THEORY IN (5+1)D: LOOPS AND MEMBRANES

In the following, we will focus on the cubic theory with  $l = m = n = 2, D = 6$ . This is a non-Abelian topological order in (5+1)D with string and membrane excitations. The strings obey Abelian fusion rule [34, 35], while the membranes are non-Abelian. Various properties of ground states and the extended operator described here will be understood from field theory later in Section IV.

#### A. Commuting non-Pauli stabilizer lattice Hamiltonian model

On each face we introduce three types of qubits for  $a_2, b_2, c_2$ , acted by Pauli operators  $X^i, Y^i, Z^i$ . Denote the  $\mathbb{Z}_2$  gauge fields  $a_2 = (1 - Z^1)/2, b_2 = (1 - Z^2)/2, c_2 = (1 - Z^3)/2$ . The commuting Hamiltonian  $H'_{\text{Cubic}}$  is given

by

$$\begin{aligned}
H'_{\text{Cubic}} = & - \sum_e \left( \prod_{\partial f \supset e} X_f^1 \right) (-1)^{\int \bar{e} \cup b_2 \cup c_2} \\
& \prod_{e'} \left( \frac{1 + (-1)^{\int \bar{e} \cup \bar{e}' \cup d c_2}}{2} \right) \prod_{e''} \left( \frac{1 + (-1)^{\int \bar{e} \cup d b_2 \cup \bar{e}''}}{2} \right) \\
& - \sum_e \left( \prod_{\partial f \supset e} X_f^2 \right) (-1)^{\int a_2 \cup \bar{e} \cup c_2} \\
& \prod_{e'} \left( \frac{1 + (-1)^{\int \bar{e}' \cup \bar{e} \cup d c_2}}{2} \right) \prod_{e''} \left( \frac{1 + (-1)^{\int d a_2 \cup \bar{e} \cup \bar{e}''}}{2} \right) \\
& - \sum_e \left( \prod_{\partial f \supset e} X_f^3 \right) (-1)^{\int a_2 \cup b_2 \cup \bar{e}} \\
& \prod_{e'} \left( \frac{1 + (-1)^{\int \bar{e}' \cup d b_2 \cup \bar{e}'}}{2} \right) \prod_{e''} \left( \frac{1 + (-1)^{\int d a_2 \cup \bar{e}'' \cup \bar{e}}}{2} \right) \\
& - \sum_c \left( \prod_{f \subset \partial c} Z_f^1 \right) - \sum_c \left( \prod_{f \subset \partial c} Z_f^2 \right) - \sum_c \left( \prod_{f \subset \partial c} Z_f^3 \right). \tag{18}
\end{aligned}$$

where  $e, f, c$  denote edges, faces and cubes. For instance, on the 5d space with coordinate  $(x, y, z, u, v)$ , the first term without the projector on the edge  $(x, y, z, u, v) = (0, 0, 0, 0, 0)$  to  $(1, 0, 0, 0, 0)$  in the  $x$  direction is given by product of  $X_f^1$  on the 16 faces that span respectively the  $\hat{x} \times (\pm \hat{y}), \hat{x} \times (\pm \hat{z}), \hat{x} \times (\pm \hat{u}), \hat{x} \times (\pm \hat{v})$  directions, where  $\hat{x}$  denotes the unit vector in the  $x$  direction. The  $(-1)^{\int \bar{e} \cup b_2 \cup c_2}$  is given by  $CZ_{f, f'}$  of the physical qubits that are acted by the Pauli operators  $X_f^2, X_{f'}^3$ , on the following pair of faces:

- $f = (x = 1, \text{Square}_{y=0, z=0}, u = v = 0)$  and  $f' = (x = 1, y = 1, z = 1, \text{Square}_{u=0, v=0})$ , where  $\text{Square}_{y=0, z=0}$  is the unit area square on the  $y, z$ -plane with four vertices  $(y, z) = (0, 0), (0, 1), (1, 0), (1, 1)$ . We note that the face  $f$  meet the edge  $(0 \leq x \leq 1, y = z = u = v = 0)$  at a single point  $(x = 1, y = z = u = v = 0)$ , the face  $f'$  does not meet this edge, and the faces  $f, f'$  meet at a single point  $(x = 1, y = 1, z = 1, u = v = 0)$ .
- The other pairs are permutations of  $y, z, u, v$ , with total  $\binom{4}{2} = 6$  pairs of  $(f, f')$  in total.

The projectors are product of the zero flux projectors  $(1 + \prod_{f'' \in \partial c} Z_{f''}^2)/2, (1 + \prod_{f''' \in \partial c'} Z_{f'''}^3)/2$  over the neighboring cubes  $c, c'$ .

## B. Ground states

Let us describe the ground state Hilbert space of the Cubic theory Hamiltonian (18). Due to the terms in

$H_{\text{Flux}}$ , the  $\mathbb{Z}_2$  gauge fields is flat within the ground state,

$$da_2 = 0, db_2 = 0, dc_2 = 0. \tag{19}$$

In addition, by multiplying the terms of  $H_{\text{Gauss}}$  over the edges crossing a closed 4d membrane in the dual lattice, we get another constraints on the  $\mathbb{Z}_2$  gauge fields within the ground state,

$$\int_{\Sigma_4} a_2 \cup b_2 = 0, \int_{\Sigma_4} a_2 \cup c_2 = 0, \int_{\Sigma_4} b_2 \cup c_2 = 0, \tag{20}$$

on any closed 4d closed membrane  $\Sigma_4$  embedded in the space. Each ground state is labeled by the configuration of the  $\mathbb{Z}_2$  gauge field satisfying the above two constraints, up to gauge equivalence.

## C. Extended operators on the lattice

### 1. Wilson surface operators

On the lattice, there are Wilson membrane operators given by product  $\prod Z_f^i$  over each small face on the closed 2d surface embedded in the space. On non-contractible 2-cycles they give rise to nontrivial logical operators.

### 2. Magnetic volume operators

There are also magnetic volume operators described by product of  $X^i$  together with projectors for each  $i$ . The projector is product  $(1 + Z^j)(1 + Z^k)$  on non-contractible 2-cycles in the volume for distinct  $j, k \neq i$  to preserve the condition (20), i.e. project out the states that will violate the condition after applying  $X^i$ . For instance, the magnetic operators for the gauge field  $c_2$  on 3-cycle  $M_3$  are

$$M^{(3)}(M_3) = P \left[ X^3(M_3^\vee) \prod_{f, f' \subset M_3} (1 + Z_f^1) (1 + Z_{f'}^2) \right] P \tag{21}$$

for distinct  $j, k \neq i$ , where  $M_3^\vee$  is the 3-cycle on the dual lattice obtained by half translating the original 3-cycle  $M_3$  by a vector  $(1/2, \dots, 1/2)$ , and  $X^3(M_3^\vee)$  is the product of  $X^3$  over faces of the original lattice crossing  $M_3^\vee$ . The term  $(1 + Z_f^1) (1 + Z_{f'}^2)$  are projectors for  $Z^1, Z^2$  support at  $M_3$ . The other magnetic operators  $M^{(1)}, M^{(2)}$  are expressed in a similar manner up to slight microscopic modification about the position of the projectors.

The projectors enforce the condition (20) evaluated on  $M_3^\vee \times M_2, M_3^\vee \times M_2'$  when the holonomy of the  $i$ th gauge field is changed on  $M_3^\vee$  ( $i = a, b, c$ ). The operator  $P$  denotes the projector onto the ground state subspace, i.e. the product of projectors for all local stabilizers along  $M_3$ . The magnetic operators commute with the Hamiltonian due to the projector, and they act on the ground



states by changing the eigenvalues of large Wilson operators.

As a consequence of the projector, the magnetic operators are non-invertible, but obey the fusion rule

$$M^{(i)}(M_3) \times M^{(i)}(M_3) = \sum_{M_2, M'_2 \in H_2(M_3)} W^{(j)}(M_2) W^{(k)}(M'_2), \quad (22)$$

for distinct  $j, k \neq i$ . Thus the magnetic volume operators describe non-Abelian membrane excitations.

We remark that another way to see the non-Abelian magnetic operator is constructing the non-Abelian Cubic Theory from  $\mathbb{Z}_2^{(2)} \times \mathbb{Z}_2^{(2)}$  2-form gauge theory of  $a_2, b_2$ , i.e. two copies of two-form toric code in (5+1)D, by gauging the  $\mathbb{Z}_2$  SPT one-form symmetry [63, 64] generated by  $(-1)^{\int a_2 \cup b_2}$ , with two-form  $\mathbb{Z}_2$  gauge field  $c_2$ . Such gauging operation couples the  $a_2, b_2$  theories. The twist defect, i.e. the magnetic defect of the gauge field  $c_2$ , lives on the boundary of such SPT and thus carries projective representation [65–67], which implies the non-Abelian fusion rule (22).

#### D. Code distance

We remark that on a hypercubic lattice with linear size  $L$  in each direction, the minimal logical operator is given by Wilson membrane operators of size  $L^2$ . The errors created by smaller size operators correspond to excited states. Thus the code distance is  $d = O(L^2) = O(N^{\frac{2}{5}})$ , where  $N = O(L^5)$  represents the total number of qubits.

### IV. CUBIC THEORY IN GENERAL DIMENSION AS NON-ABELIAN TQFT

#### A. Field Theory

Here we describe the gauge theory that describes the Cubic theory in  $D$  spacetime dimensions. Consider  $\mathbb{Z}_2$   $l$ -form,  $m$ -form and  $n$ -form gauge fields  $a_l, b_m, c_n$  satisfying  $l + m + n = D$ , with the action

$$\pi \int a_l \cup b_m \cup c_n. \quad (23)$$

We can write the theory by embedding the gauge fields into  $U(1)$  gauge fields:

$$\frac{1}{\pi^2} \int a_l b_m c_n + \frac{2}{2\pi} \int (a_l d\tilde{a}_{D-l-1} + b_m d\tilde{b}_{D-m-1} + c_n d\tilde{c}_{D-n-1}). \quad (24)$$

Examples of the theory are discussed in various literature:

- When  $l = 1, m = 1$ , the gauge fields  $(a_1, b_1, \tilde{c}_1)$  describe the gauge field of  $\mathbb{D}_8$  one-form gauge theory: the equation of motion for  $c_{D-2}$  sets  $d\tilde{c}_1 = \frac{1}{\pi} a_1 b_1$ , which described the extension of  $\mathbb{Z}_2 \times \mathbb{Z}_2$  by  $\mathbb{Z}_2$

with the 2-cocycle given by  $a_1 b_1$ . When  $D = 3$ , the equivalence with the  $\mathbb{D}_8$  gauge theory is discussed in e.g. [68–70].

- When  $l = 2, m = 2$ , and  $D = 5$ , this is gauging the  $\mathbb{Z}_2$  0-form symmetry of the (4+1)D 2-form  $\mathbb{Z}_2^2$  gauge theory

$$\frac{2}{2\pi} \int (a_2 d\tilde{a}_2 + b_2 d\tilde{b}_2) \quad (25)$$

generated by the toric code Walker Wang domain wall with the generator given by  $\exp(\frac{i}{\pi} \int a_2 b_2)$ .

#### B. Hilbert space of TQFT

The equation of motions are (here we normalize the gauge fields to have holonomy  $0, \pi$  as in (24))

$$\begin{aligned} da_l &= 0, & db_m &= 0, & dc_n &= 0 \\ d\tilde{a}_{D-l-1} + b_m c_n / \pi &= 0, \\ d\tilde{b}_{D-m-1} + a_l c_n / \pi &= 0, \\ d\tilde{c}_{D-n-1} + a_l b_m / \pi &= 0. \end{aligned}$$

Thus the Hilbert space of the TQFT on a spatial manifold can be described by holonomies of  $a_l, b_m, c_n$  subject to the constraints (below we use the normalization that the holonomies are  $0, 1 \pmod{2}$ )

$$a_l \cup b_m = 0, \quad a_l \cup c_n = 0, \quad b_m \cup c_n = 0. \quad (26)$$

We note that the constraints on the  $\mathbb{Z}_2$  gauge fields described above reproduces those on the ground state of the Cubic Theory Hamiltonian derived in Section III B.

#### C. Operators

The theory has the following topological operators: (here we normalize the gauge fields to have holonomy  $0, \pi$  as in (24))

- The theory has invertible operators generated by the electric Wilson operators

$$W^{(1)} = e^{i \int a_l}, \quad W^{(2)} = e^{i \int b_m}, \quad W^{(3)} = e^{i \int c_n}. \quad (27)$$

The electric Wilson operators obey  $\mathbb{Z}_2^3$  fusion rule.

- The magnetic operators are

$$\begin{aligned} & e^{i \int_{\Sigma_{D-l-1}} \tilde{a}_{D-l-1} + i \int_{\mathcal{V}_{D-l}} b_m c_n / \pi} \\ & e^{i \int_{\Sigma_{D-m-1}} \tilde{b}_{D-m-1} + i \int_{\mathcal{V}_{D-m}} a_l c_n / \pi} \\ & e^{i \int_{\Sigma_{D-n-1}} \tilde{c}_{D-n-1} + i \int_{\mathcal{V}_{D-n}} a_l b_m / \pi}, \end{aligned} \quad (28)$$

where  $\Sigma_k = \partial\mathcal{V}_{k+1}$ . Since in the Hilbert space  $a_l \cup b_m = 0$ ,  $a_l \cup c_n = 0$ ,  $b_m \cup c_n = 0$ , these operators do not depend on the choice of  $\mathcal{V}_i$  bounded by  $\Sigma_{i-1}$  for  $i = D-l, D-m, D-n$ , respectively [63]. To obtain magnetic operators without  $\mathcal{V}_{k+1}$ , we can put choose a local polarization [71–74], i.e. consider  $\mathcal{V}_{k+1}$  with two boundaries, one with magnetic operators, the other a topological boundary condition. The topological boundary condition can be described by a normal subgroup  $H$  of the bulk gauge group such that the topological action on  $\mathcal{V}_{k+1}$  becomes trivial, i.e. well-defined boundary without gauge anomalies, and a topological action on the boundary for the  $H$  subgroup.

For instance, we can obtain a magnetic operator for  $a_l$  on  $\Sigma_{D-l-1}$  by choosing the other topological boundary to be  $b_m| = c_n| = 0$ , which gives a magnetic operator decorated with the condensation of the Wilson operators  $W^{(2)}, W^{(3)}$  on  $\Sigma_{D-l-1}$  that imposes the projection to  $b_m| = 0, c_n| = 0$  [75]. We will call such magnetic operator  $M^{(1)}$ , and similarly define  $M^{(2)}, M^{(3)}$  using the Dirichlet boundary conditions of  $(a_l, c_n), (a_l, b_m)$ , respectively.

From the condensate of Wilson operators, one can derive the non-Abelian fusion rules (see also [63])

$$\begin{aligned} M^{(I)} \times W^{(J)} &= M^{(I)}, I \neq J \\ M^{(I)} \times M^{(I)} &= \sum W^{(J)}(\gamma)W^{(K)}(\gamma'), \end{aligned} \quad (29)$$

for distinct  $I, J, K$ . In particular, the fusion rule in the second equation corresponds to that of the magnetic operators in the lattice model (22).

- Gauged symmetry-protected topological (SPT) operators [48, 63, 76–78]  $H^*(B^l\mathbb{Z}_2 \times B^m\mathbb{Z}_2 \times B^n\mathbb{Z}_2, U(1))$ . The closed gauged SPT operators  $\int a_l b_m, \int a_l c_n, \int b_m c_n$  are trivial. There are following nontrivial gauged SPT operators:

$$\begin{aligned} V^{12} &= e^i \int a_l db_m / (2\pi), \\ V^{23} &= e^i \int b_m dc_n / (2\pi), \\ V^{13} &= e^i \int a_l dc_n / (2\pi). \end{aligned} \quad (30)$$

- “Mixed” operators that involve the electric and the

magnetic operators:

$$\begin{aligned} e^i \int_{\partial M_{D-m+l}} a_l \tilde{b}_{D-m-1/\pi+i} \int_{M_{D-m+l}} a_l^2 c_n / \pi^2 \\ e^i \int_{\partial M_{D-l+m}} b_m \tilde{a}_{D-l-1/\pi+i} \int_{M_{D-m+l}} b_m^2 c_n / \pi^2 \\ e^i \int_{\partial M_{D-n+m}} b_m \tilde{c}_{D-n-1/\pi+i} \int_{M_{D-n+m}} b_m^2 a_l / \pi^2 \\ e^i \int_{\partial M_{D-m+n}} c_n \tilde{b}_{D-m-1/\pi+i} \int_{M_{D-m+n}} c_n^2 a_l / \pi^2 \\ e^i \int_{\partial M_{D-l+n}} c_n \tilde{a}_{D-l-1/\pi+i} \int_{M_{D-l+n}} c_n^2 b_m / \pi^2 \\ e^i \int_{\partial M_{D-n+l}} a_l \tilde{c}_{D-n-1/\pi+i} \int_{M_{D-n+l}} a_l^2 b_m / \pi^2 \end{aligned} \quad (31)$$

As in the magnetic operators, these operators do not depend on the bulk. To define operators without using the bulk, we can choose a local polarization by putting the operator on one boundary and a topological boundary condition on the other boundary. For instance, in the first operator we can impose the Dirichlet boundary conditions for  $a_l, c_n$ , and similar for the other operators. Let us call the resulting operators on the boundary  $\mathcal{D}^{12}, \mathcal{D}^{21}, \mathcal{D}^{23}, \mathcal{D}^{32}, \mathcal{D}^{31}, \mathcal{D}^{13}$ . Due to the condensate from the topological boundary conditions, the operators  $\mathcal{D}^{ij}$  are non-invertible.

The operators act on the Wilson and magnetic operators. For instance, when the Wilson operator  $W^{(2)}$  intersects  $\mathcal{D}^{12}$ , it creates holonomy for  $\tilde{b}_{D-m-1}$ , and results in additional Wilson operator  $W^{(1)}$ . On the other hand, when the magnetic operator  $M^{(1)}$  intersects  $\mathcal{D}^{12}$ , the projectors for  $W^{(1)}$  annihilate the magnetic operator, and similarly for  $M^{(3)}$ . In other words, the magnetic operators  $M^{(1)}, M^{(3)}$  cannot intersect with or terminate at  $\mathcal{D}^{12}$ :

$$\begin{aligned} \mathcal{D}^{12}: \quad W^{(1)} &\rightarrow W^{(1)}, \quad W^{(2)} \rightarrow W^{(1)}W^{(2)}, \\ M^{(1)} &\rightarrow 0, \quad M^{(3)} \rightarrow 0. \end{aligned} \quad (32)$$

#### D. Cubic theories without particles

Let us consider the class of cubic theories that do not have particles. In other words, all gauge fields  $a, b, c, \tilde{a}, \tilde{b}, \tilde{c}$  have degree greater or equal 2. This requires

$$\begin{aligned} l \geq 2, \quad m \geq 2, \quad n \geq 2, \\ D-l-1 \geq 2, \quad D-m-1 \geq 2, \quad D-n-1 \geq 2. \end{aligned} \quad (33)$$

These conditions simplify to

$$l \geq 2, \quad m \geq 2, \quad n \geq 2. \quad (34)$$

This inequality gives  $l + m + n = D \geq 6$ . The condition on spacetime dimension  $D$  is consistent with the no-go

theorem for non-Abelian TQFTs without particles. The inequality is saturated with  $D = 6, l = m = n = 2$ . For every spacetime dimension  $\geq 6$ , there is a non-Abelian TQFT without particles given by the Cubic theory.

As a consistency check, we note that in theories without particles, since the electric excitations obey Abelian fusion rule and magnetic excitations obey non-Abelian fusion rules, the dimensions of the magnetic excitations must be strictly greater than the minimal dimension of the electric excitations due to the constraint discussed in appendix A (see also [34, 35]):

$$\begin{aligned} D - l - 1 &> \min(l, m, n) \\ D - m - 1 &> \min(l, m, n) \\ D - n - 1 &> \min(l, m, n) . \end{aligned} \quad (35)$$

In such case, we can use electric excitations to form condensate whose dimension is one less than that of the magnetic excitations. Since there are condensates of all dimensions down to the dimension of the electric excitation itself which obeys Abelian fusion rules, the condition in appendix A follows from (35). On the other hand, we can reproduce the conditions (35) from the inequalities in (34) for the cubic theories without particles. The inequalities of (35) are related by permutation of  $l, m, n$ , so without loss of generality we can consider the first one of them; suppose the minimum on the right hand side is  $l$  (including the case when the minimum is degenerate), then  $(D - l - 1) > l$  follows from  $m \geq n$  and  $n \geq 2$  in (34).

Thus the theories without particles have the properties that the lowest dimensional excitations obey Abelian fusion rule, in agreement with constraint on excitations with non-Abelian fusion rules (see e.g. appendix A).

## V. CUBIC THEORY IN (5+1)D AS NON-ABELIAN TQFT

In the following, we will continue the discussions on the properties of Cubic theory, focusing on  $l = m = n = 2, D = 6$ . We will describe the braiding of non-Abelian magnetic operators.

### A. TQFT Hilbert space

The equation of motion implies

$$a_2 \cup b_2 = 0, \quad a_2 \cup c_2 = 0, \quad b_2 \cup c_2 = 0 . \quad (36)$$

The Hilbert space is described by different holonomies of the two-form  $\mathbb{Z}_2$  gauge fields  $a_2, b_2, c_2$  subject to the above constraint.

For instance, suppose the space is  $S^2 \times S^2 \times S^1$ . Denote the holonomies on the two  $S^2$ s by the three-component vectors  $\vec{n}_i = (n_i^a, n_i^b, n_i^c)$  with  $n_i^a = 0, 1 \pmod 2$  is the holonomy of  $a_2$  on the  $i$ th  $S^2$ , the constraint is

$$\vec{n}_1 \times \vec{n}_2 = 0 \pmod 2 . \quad (37)$$

There are 22 solutions, thus the Hilbert space of the TQFT on  $S^2 \times S^2 \times S^1$  has dimension 22.

### B. Operators

There are Wilson surface operators

$$W^{(1)} = e^i \int a_2, \quad W^{(2)} = e^i \int b_2, \quad W^{(3)} = e^i \int c_2 . \quad (38)$$

The integral is over the support of the Wilson surface, given by 2-cycles  $M_2$ . The Wilson surface operators obey  $\mathbb{Z}_2^3$  fusion rule. Under union of surfaces, the Wilson operators satisfy  $W^{(i)}(M_2) \times W^{(i)}(M'_2) = W^{(i)}(M_2 + M'_2)$  for any two 2-cycles  $M_2, M'_2$ . On the lattice, they are described by product of  $Z^i$  for each  $i$ . The Wilson surface operators correspond to string excitations, and they obey  $\mathbb{Z}_2^3$  fusion rules.

There are magnetic volume operators

$$\begin{aligned} M^{(1)} &= e^i \int \tilde{a}_3 + i \int b_2 c_2 / \pi, \\ M^{(2)} &= e^i \int \tilde{b}_3 + i \int a_2 c_2 / \pi, \\ M^{(3)} &= e^i \int \tilde{c}_3 + i \int a_2 b_2 / \pi . \end{aligned} \quad (39)$$

The integral is over the support of the volume operators, given by 3-cycles  $M_3$ .

### C. Non-Abelian braiding of magnetic operators

#### 1. Two-membrane braiding gives 0

The magnetic operators obey non-Abelian braiding following the method of [63]. The braiding can be derived from the commutator of the non-invertible operators (21). Consider the correlation function of two different magnetic operators

$$\langle M^{(1)}(V_3) M^{(2)}(V'_3) \rangle . \quad (40)$$

The equation of motion for  $\tilde{a}_3, \tilde{b}_3$  sets  $da_2 = -\pi\delta(V_3)^\perp, db_2 = -\pi\delta(V'_3)^\perp$ , where  $\delta(V_3)^\perp$  is a delta function 3-form that restricts integrals to  $V_3$ . For  $V_3 = \partial V_4, V'_3 = \partial V'_4$  this reduces to  $a_2 = -\pi\delta(V_4)^\perp, b_2 = -\pi\delta(V'_4)^\perp$ . We are left with

$$e^i \int c_2 \delta(V_4)^\perp \delta(V'_4)^\perp . \quad (41)$$

The equation of motion for  $c_2$  sets  $d\tilde{c}_3 = \pi\delta(V_4)^\perp \delta(V'_4)^\perp$ . For non-exact  $\delta(V_4)^\perp \delta(V'_4)^\perp$  the equation does not have a solution, and thus the correlation function is zero. Another way to see the correlation function is zero is by performing path integral over  $\mathbb{Z}_2$  gauge field  $c_2$ , whose possible holonomy is  $0, \pi \pmod{2\pi}$ : for the configuration where  $\int c_2 \delta(V_4)^\perp \delta(V'_4)^\perp = 0, \pi$ , the correlation function is

$$e^{0i} + e^{\pi i} = 0 . \quad (42)$$

Such vanishing correlation function indicates the magnetic operators are non-Abelian. This generalizes the vanishing Hopf braiding of two non-Abelian particles in (2+1)D  $\mathbb{D}_8$  gauge theory (see e.g. [69]). This is similar to the braiding of non-Abelian Ising anyon. The above computation indicates that there are two braiding channels.

In the lattice model on periodic space of  $T^5$  topology, consider the commutator of the magnetic operators  $M^{(1)}(T_{1,2,3}^3), M^{(2)}(T_{1,4,5}^3)$  supported on two 3-tori with subscripts labelling the coordinates, where

$$\begin{aligned} M^{(1)}(T_{1,2,3}^3) &= P \left[ X^1(T_{1,2,3}^{3\vee}) \prod_{f,f' \subset T_{1,2,3}^3} (1 + Z_f^2) (1 + Z_{f'}^3) \right] P \\ &= P X^1(T_{1,2,3}^{3\vee}) \prod_{f,f' \subset T_{1,2,3}^3} (1 + Z_f^2) (1 + Z_{f'}^3) \\ &\quad \times \left( \frac{1 + Z^2(T_{2,3}^2)}{2} \right) P \\ M^{(2)}(T_{1,4,5}^3) &= P \left[ X^1(T_{1,4,5}^{3\vee}) \prod_{f,f' \subset T_{1,4,5}^3} (1 + Z_f^2) (1 + Z_{f'}^3) \right] P, \end{aligned} \quad (43)$$

where  $Z^2(T_{2,3}^2)$  is the product of  $Z_f^2$  over the 2-torus  $T_{2,3}^2$ . From the above expressions we find

$$\begin{aligned} &M^{(1)}(T_{1,2,3}^3) M^{(2)}(T_{1,4,5}^3) \\ &= M^{(1)}(T_{1,2,3}^3) M^{(2)}(T_{1,4,5}^3) \cdot \frac{1 - Z^2(T_{2,3}^2)}{2} \end{aligned} \quad (44)$$

due to the anti-commutation relation between  $Z^2(T_{2,3}^2)$  and  $X^1(T_{1,4,5}^{3\vee})$ . Meanwhile we have

$$\begin{aligned} &M^{(1)}(T_{1,2,3}^3) M^{(2)}(T_{1,4,5}^3) \\ &= \frac{1 + Z^2(T_{2,3}^2)}{2} \cdot M^{(1)}(T_{1,2,3}^3) M^{(2)}(T_{1,4,5}^3). \end{aligned} \quad (45)$$

The braiding can then be obtained as

$$M^{(1)}(T_{1,2,3}^3) M^{(2)}(T_{1,4,5}^3) M^{(1)}(T_{1,2,3}^3) M^{(2)}(T_{1,4,5}^3) = 0, \quad (46)$$

which follows from  $(1 - Z^2(T_{2,3}^2))(1 + Z^2(T_{2,3}^2)) = 0$ , i.e.  $M^{(1)}(T_{1,2,3}^3) M^{(2)}(T_{1,4,5}^3)$  and  $M^{(2)}(T_{1,4,5}^3) M^{(1)}(T_{1,2,3}^3)$  have orthogonal projectors.

#### D. ‘‘Borromean rings’’ braiding of membranes

If we include additional magnetic operator  $M^{(3)}(V_3'')$ , i.e. correlation function of  $M^{(1)}(V_3), M^{(2)}(V_3'), M^{(3)}(V_3'')$ , the new magnetic operator sources the holonomy of  $c_2 = -\pi\delta(V_4'')$  with  $\partial V_4'' = V_3''$ , thus the three magnetic operators have the correlation function

$$(-1)^{\int \delta(V_4) \delta(V_4') \delta(V_4'')} . \quad (47)$$

The correlation gives  $(-1)$  for the three volume operators arranged in analogue of Borromean rings. The discussion is similar to the  $D = 3, m = n = 1$  case in [79]. See Fig. 4 for illustrations in the (2+1)D model. Therefore the non-Abelian membrane excitations, just like the non-Abelian excitations in the  $\mathbb{D}_8$  topological orders, enjoy nontrivial Borromean ring type braiding given by a sign, which does not have any pairwise braiding of the membrane excitations—this implies that the process cannot be realized in Abelian topological orders.

## VI. CUBIC THEORY FROM COMPACTIFYING GENERALIZED COLOR CODE

The cubic theory in  $D$  spacetime dimensions can be obtained from twisted compactification of a generalized color code theory in  $(D + 1)$  spacetime dimensions [5, 80], where the generalized color code theory is equivalent to decoupled  $\mathbb{Z}_2$   $l$ -form gauge theory,  $\mathbb{Z}_2$   $m$ -form gauge theory and  $\mathbb{Z}_2$   $n$ -form gauge theory.

The  $(D + 1)$ -dimensional theory can be described by three copies of  $\mathbb{Z}_2$  toric code with qubits on spatial  $l$ -hypercubes,  $m$ -hypercubes and  $n$ -hypercubes, respectively. It is equivalent to a single copy of generalized color code up to a constant-depth local quantum circuit (see e.g. [5, 80, 81]). For example, the  $D = 6, l = m = n = 2$  case corresponds to the color code in 6d space, which is a self-correcting memory described in Ref. [5]. This gives rise to our non-Abelian self-correcting memory in five spatial dimensions after the twisted compactification process.

The  $(D + 1)$  dimensional theory has a  $\mathbb{Z}_2$  0-form symmetry generated by gauged SPT defect (denoted by  $s^{(3)}$ ) [48, 63, 76–78] given by domain wall decorated with the topological action (23). If the space is  $S^l \times S^m \times S^n$ , the  $\mathbb{Z}_2$  0-form symmetry acts as a constant-depth circuit composed of the product of CCZ gates on the triplet of qubits in three copies of toric codes respectively, which is dual to the transversal  $T$  gate in the generalized color code [80]. The corresponding symmetry operator in the TQFT can be expressed as:

$$\mathcal{D}_{s^{(3)}}(M_D) = \exp \left( \pi i \int_{M_{D+1}} a_l \cup b_m \cup c_n \right), \quad (48)$$

where for the  $D = 3, l = m = n = 1$  case the correspondence to the CCZ gates in three copies of 3D toric codes has been discussed in Ref. [48, 78] and the correspondence to the transversal  $T$  gates in the 3D color code can be found in Ref. [23].

We note that when a magnetic defect of one gauge field pierces the domain wall  $s^{(3)}$ , it forms a junction with the domain wall that has the non-Abelian magnetic defect in the cubic theory, whose fusion produces the Wilson operators for the other two  $\mathbb{Z}_2$  gauge fields. This gives an operator-value associator similar to the junction discussed in section 2.3 of [64].

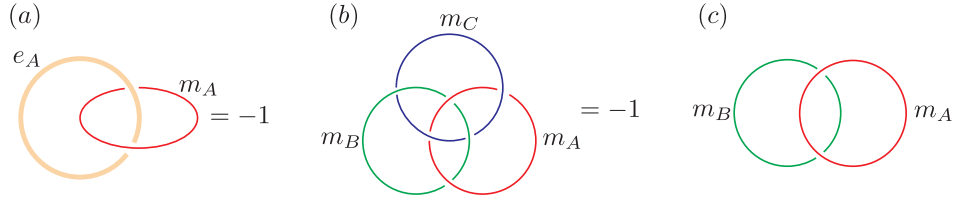


FIG. 4. Illustration of the braiding process in (2+1)D space-time. (a). Mutual braiding phase ( $e^{i\pi} = -1$ ) of the  $e_A$  and  $m_A$  particles in the copy  $A$  of the (2+1)D  $\mathbb{D}_8$  topological order. (b). The Borromean ring braiding phase of the  $m_A$ ,  $m_B$ , and  $m_C$  particles in the (2+1)D  $\mathbb{D}_8$  topological order. This braiding process can also be generalized to the (5+1)D where the  $m$ -excitation becomes 2D membrane. (c). In the absence of the worldline of  $m_C$ , there is no linking between the worldlines of  $m_A$  and  $m_B$  which leads to a trivial phase between them.

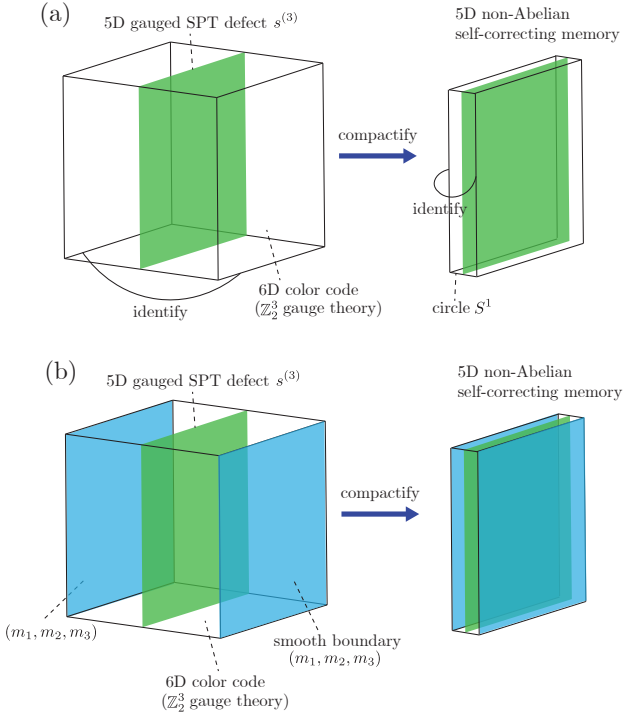


FIG. 5. Non-Abelian self-correcting memory from (a) compactification of color code on a circle with gauged SPT defect inserted, and (b) reduction on an interval with  $m$ -condensed boundaries (i.e. Neumann boundary conditions for the higher-form  $\mathbb{Z}_2$  gauge fields) on two ends and the gauged SPT defect inserted in the middle.

The twisted compactification of the  $(D + 1)$ -dimensional theory to  $D$  spacetime dimensions is given by turning on holonomy of this  $\mathbb{Z}_2$  0-form symmetry along the internal circle direction, i.e. placing the domain wall at a point on the circle, and we keep only the zero modes of the gauge fields  $a_l, b_m, c_n$  that do not wind around the

circle.<sup>4</sup> The holonomy introduce the action

$$\pi \int a_l \cup b_m \cup c_n \cup (d\theta/2\pi), \quad (49)$$

where  $\theta \sim \theta + 2\pi$  is the coordinate of the circle, and this corresponds to the background gauge field  $d\theta/2\pi$  for the  $\mathbb{Z}_2$  0-form symmetry. Integrating over the circle direction gives the topological action (23). Alternatively, we can reduce the  $(D + 1)$ -dimensional theory on an interval with Neumann boundary condition for the gauge fields and the  $\mathbb{Z}_2$  domain wall in the middle. The Neumann boundary conditions for the gauge fields correspond to the  $m$ -condensed or smooth boundaries. See Figure 5 for an illustration.

We remark that similar twisted dimensional reduction for twisted gauge theory in  $D = 3$  is discussed in [70].

## VII. SELF-CORRECTING QUANTUM MEMORY

### A. Interaction between system and environment

To describe the self correcting quantum memory, we will model the interaction between the system and environment using Lindbladian evolution following e.g. [50]. We will assume the total Hilbert space factorizes into the tensor product of the system Hilbert space and the environment Hilbert space. The total system including the environment (“the bath”) has the Hamiltonian

$$H = H_{\text{sys}} + H_{\text{env}} + H_{\text{int}}, \quad (50)$$

where  $H_{\text{sys}}, H_{\text{env}}, H_{\text{int}}$  are the Hamiltonians for the system, the environment, and interaction, respectively. The interaction Hamiltonian takes the form

$$H_{\text{int}} = \sum_{\alpha} S_{\alpha} \otimes f_{\alpha}, \quad (51)$$

<sup>4</sup> The winding modes will give additional  $(l-1)$ -form,  $(m-1)$ -form and  $(n-1)$ -form gauge fields  $\int a_l, \int b_m, \int c_n$ .



where  $S_\alpha, f_\alpha$  act on the system Hilbert space and environment Hilbert space, respectively. We can evolve a general operator using the total Hamiltonian and then trace out the environment Hilbert space. This results in effective Lindbladian evolution for an operator  $O$  in Heisenberg picture: [50]

$$\begin{aligned} \frac{dO}{dt} &= \mathcal{L}[O], \\ \mathcal{L} &= i[H_{\text{sys}}, O] + \frac{1}{2} \sum_{\alpha} \sum_{\omega} (h_{\alpha}(\omega) (S_{\alpha}^{\dagger}(\omega)[O, S_{\alpha}(\omega)] \\ &\quad + [S_{\alpha}^{\dagger}(\omega), O]S_{\alpha}(\omega))) , \end{aligned} \quad (52)$$

where  $S_{\alpha}(\omega)$  is the Fourier transform of  $S_{\alpha}(t) := e^{iH_{\text{sys}}t} S_{\alpha} e^{-iH_{\text{sys}}t}$ , and  $h_{\alpha}(\omega)$  is the Fourier transform of the autocorrelator of  $f_{\alpha}$ . We will assume  $h_{\text{max}} := \sup_{\alpha, \omega \geq 0} h_{\alpha}(\omega)$  is finite [50].

From [50], the decay rate of a logical operator  $O$  in the Heisenberg picture under the system Hamiltonian dressed by the error-correcting map onto the ground state is defined as

$$-\langle O, \mathcal{L}(O) \rangle_{\beta} := -\text{Tr}(\rho_{\beta} O^{\dagger} \mathcal{L}(O)) , \quad (53)$$

where  $\rho_{\beta}$  is the thermal equilibrium density matrix at temperature  $1/(\beta k_B)$ . Provided that  $-\langle O, \mathcal{L}(O) \rangle_{\beta} \leq \epsilon$ , the decay of the operator is upper bounded as

$$\langle O, O(t) \rangle_{\beta} \geq e^{-\epsilon t}. \quad (54)$$

As shown in [50], for finite  $h_{\text{max}}$  the upper bound of the decay rate  $\epsilon$  can be given by the Boltzmann probability of the error syndrome, i.e. excitation pattern, that is critical for the logical operator  $O$ , i.e. single-qubit error that changes the value of  $O$  (see discussions around Eq. (67) for details)

$$P_{\text{crit } O} = \frac{\sum_{\text{critical}} e^{-\beta E}}{\sum_{\text{all error}} e^{-\beta E(\text{error})}} . \quad (55)$$

For a given temperature, if the above Boltzmann probability is exponentially small on the size of the system, we say that the logical operator is stable. The discussion can be separated into two steps: [50] (1) show that with high probability only configurations for small excitations appear in the Gibbs state. This is determined by the competition between the Boltzmann weight, and the entropy effect that counts the number of excitation patterns with the same energy. (2) Show that the configurations with only small (contractible) excitations are not critical, i.e. a single spin flip will not change the value of dressed observable. The second step essentially means that small excitations whose size is less than the code distance can be corrected, while the first step is more nontrivial and it gives the critical temperature for the quantum memory. We will investigate it in more details in section VII B.

### 1. Pauli noise model

Let us first illustrate the above formalism using concrete Pauli noise model, following [50]. The Pauli noise

model is widely used and can describe practical noises in quantum computers [82]. Consider the Cubic theory Hamiltonian coupled to the environment,

$$H = H_{\text{sys}} + H_{\text{env}} + H_{\text{int}} , \quad (56)$$

where

$$H_{\text{sys}} = H'_{\text{Cubic}} . \quad (57)$$

We consider the coupling to the environment in the form of

$$H_{\text{int}} = \sum_{j,k} X_k^j \otimes f_{j,k} + \sum_{j,k} Y_k^j \otimes g_{j,k} + \sum_{j,k} Z_k^j \otimes h_{j,k} , \quad (58)$$

where the sum over  $j$  runs  $j = 1, 2, 3$  and  $k$  runs over all sites. For simplicity, it is written as

$$H_{\text{int}} = \sum_{\sigma} \sigma \otimes f_{\sigma} , \quad (59)$$

where the sum over  $\sigma$  runs over all Pauli  $X^j, Y^j, Z^j$  matrices on a single site.

The Cubic theory Hamiltonian with the above coupling is subject to Pauli errors. The  $X$ -error leads to the error syndrome of  $H_{\text{Flux}}$ , characterized by  $\pm 1$  eigenvalues of the terms of  $H_{\text{Flux}}$ . These eigenvalues are represented by the vector  $\mathbf{b}^X \in \mathbb{Z}_2^{3|c|}$ .

The  $Z$ -error causes the syndrome of  $H'_{\text{Gauss}}$ . Due to the presence of the projector onto the zero flux sector, the eigenvalues of the terms in  $H'_{\text{Gauss}}$  becomes either  $1, 0, -1$ . In order to express the error syndrome in terms of the  $\mathbb{Z}_2$  vector as in the case of the  $Z$ -error, one first needs to correct the  $X$ -errors by acting suitable Pauli  $X$  operators. After the correction we have  $\mathbf{b}^X = 0$ . The  $Z$ -error is then characterized by the vector  $\mathbf{b}^Z \in \mathbb{Z}_2^{3|e|}$ , which is the  $\pm 1$  eigenvalues of the terms of  $H'_{\text{Gauss}}$ .

Once the above sequential procedure of error correction is understood, the error syndrome of this model can be expressed by a pair of vectors

$$\mathbf{b} = \{\mathbf{b}^X, \mathbf{b}^Z\} , \quad (60)$$

where  $\mathbf{b}^X \in \mathbb{Z}_2^{3|c|}$ .

For a given stabilizer state in the presence of the errors  $\mathbf{b}$ , we define a recovery map that corrects the error, which is in the form of

$$\text{corr}(\mathbf{b}) = \text{corr}_{\text{Gauss}}(\mathbf{b}^Z) \text{corr}_{\text{Flux}}(\mathbf{b}^X) . \quad (61)$$

This map corrects the  $X$ -error first, and then  $Z$ -error next. Concretely,

$$\text{corr}_{\text{Flux}} : \mathbb{Z}_2^{3|c|} \rightarrow \mathcal{P}_X , \quad (62)$$

where  $\text{corr}_{\text{Flux}}(\mathbf{b}^X)$  is a product of  $X^1, X^2, X^3$  that recovers the syndrome of the  $H_{\text{Flux}}$ . Also

$$\text{corr}_{\text{Gauss}} : \mathbb{Z}_2^{3|e|} \rightarrow \mathcal{P}_Z , \quad (63)$$

where  $\text{corr}_{\text{Gauss}}(\mathbf{b}^Z)$  is a product of  $Z^1, Z^2, Z^3$  that recovers the syndrome of the  $H_{\text{Gauss}}$ .

In the presence of the error, we consider the dressed logical operators

$$O_{\text{dr}} = \sum_{\mathbf{b}} \text{corr}(\mathbf{b})^\dagger O \text{corr}(\mathbf{b}) P_{\mathbf{b}}, \quad (64)$$

where  $O$  is the logical operator of the stabilizer state without errors.  $P_{\mathbf{b}}$  is the projection onto the stabilizer state in the presence of the error  $\mathbf{b}$ . The thermal stability of the quantum memory is verified by checking if the decay rate of the dressed logical operators  $O_{\text{dr}}$  becomes exponentially small with respect to the system size, at nonzero low temperature.

For any Pauli operator  $E \in \mathcal{P}$  and an error syndrome  $\mathbf{b}$ , the commutation relation between  $O_{\text{dr}}$  and  $E$  becomes a number

$$O_{\text{dr}} E P_{\mathbf{b}} = S(O, E, \mathbf{b}) E O_{\text{dr}} P_{\mathbf{b}}, \quad (65)$$

where  $S(O, E, \mathbf{b}) = \pm 1$ . If there exists a single Pauli error  $\sigma$  satisfying  $S(O, E, \mathbf{b}) = 1$ , the error  $\mathbf{b}$  is said to be  $O$ -critical. That is, the logical operator  $O_{\text{dr}}$  in the presence of the  $O$ -critical error changes its value by an additional single-qubit error.

Let us then obtain the upper bound on the decay rate. We use the inequality

$$-\langle A, \mathcal{L}(A) \rangle_\beta \leq 2\hat{h}_{\text{max}} \sum_{\sigma} \langle [\sigma, A], [\sigma, A] \rangle_\beta. \quad (66)$$

Using (65), (66) one can derive the upper bound of the decay rate as

$$\begin{aligned} -\langle O_{\text{dr}}, \mathcal{L}(O_{\text{dr}}) \rangle_\beta &\leq 4\hat{h}_{\text{max}} \frac{\sum_{\mathbf{b}, \sigma} e^{-\beta E_{\mathbf{b}}} (1 - S(O, \sigma, \mathbf{b}))}{\sum_{\mathbf{b}} e^{-\beta E_{\mathbf{b}}}} \\ &\leq 8\hat{h}_{\text{max}} n P_{\text{crit}_O}. \end{aligned} \quad (67)$$

Here,  $P_{\text{crit}_O}$  is the probability of finding the  $O$ -critical errors, i.e. the errors  $\mathbf{b}$  where one can find a single qubit error  $\sigma$  such that  $S(O, \sigma, \mathbf{b}) = -1$ .  $n$  is the number of physical qubits.

## 2. Stability against small excitations

As mentioned in Sec. VII A, to achieve thermal stability of the quantum memory it is required that the small excitations are not critical for any logical operators. This can be satisfied by making an appropriate choice of the correction maps  $\text{corr}(\mathbf{b})$  so that the small syndromes (say within the region  $R$  of the size  $\xi L$  for the system size  $L$  and a constant  $\xi$ ) disconnected from other syndromes is corrected by the Pauli operators within the region  $R$ .

## B. Self-correcting quantum memory with loops and membranes

Let us analyze the self-correcting property for the model on 5-dimensional hypercubic spatial lattice. The Hamiltonian model in section III with  $l = m = n = 2, D = 6$  has Gauss law term for each edge and flux term for each cube, and each face has 3 types of qubits for  $a, b, c$ .

Since we have a commuting (non-Pauli) stabilizer models in Eq. (17), the errors inducing the loop and membrane excitations can be decoupled and corrected independently, similar to the 4d self-correcting toric-code case where the e-excitations induced by the Z-type errors and m-excitations induced by the X-type errors can be corrected independently. Thus, we will apply a similar analysis using a Peierls argument as in Ref. [1] for the 4d toric code.

We consider the quantum memory being coupled to a thermal bath with temperature  $T$  and focus on the thermal noise since its not correctable for usual topological memories without self-correction capability.

*a. Errors inducing loop excitations* We first discuss correction of the errors inducing loop excitations. The unit-time probability for creation or survival of a small loop excitation on a plaquette, i.e. violating the Gauss term on the 4 boundary edges, is given by the Boltzmann ratio:

$$\frac{P(0 \rightarrow 4)}{P(0 \rightarrow 0)} = \frac{P(4 \rightarrow 4)}{P(4 \rightarrow 0)} = e^{-8\beta} \quad (\beta = 1/T), \quad (68)$$

where the energy cost along each edge is taken to be 2 (flipping  $-1$  to  $+1$  in the Gauss law term) and  $P(i \rightarrow j)$  stands for the unit-time transition probability (rate) from  $i$  violated edges to  $j$  violated edges. Note that both transition processes  $0 \rightarrow 4$  and  $4 \rightarrow 0$  can be induced by a ‘‘plaquette flipping’’ corresponding to a Pauli-Z operator  $Z_f$  acted on the qubit associated with the plaquette  $f$ . Similarly, the transition process between the configurations with 1 violated edge and 3 violated edges is also induced by a plaquette flipping, with the transition probability ratio given by:

$$\frac{P(1 \rightarrow 3)}{P(1 \rightarrow 1)} = \frac{P(3 \rightarrow 3)}{P(3 \rightarrow 1)} = e^{-4\beta}. \quad (69)$$

Finally, for all the configurations with two violated edges which have the same energy, one can set the plaquette flipping probability at unit time to be  $1/2$  which connects different configurations and ensures ergodicity (any initial configuration has a non-zero probability to reach any final configuration). As one can see, when the temperature  $T$  (and the thermal noise) is low enough, such local system-bath interaction will gradually shrink the perimeter of the loop excitations and suppress the error proliferation autonomously. This prevents a homologically non-trivial worldsheets of loop excitations being created which induces a logical error.

The critical temperature below which the loop excitation error is self-correcting is determined by the balance between the Boltzmann suppression  $e^{-2\beta\ell}$  for loop of length  $\ell$  and the loop entropy. The latter can be estimated from the self-avoiding random walk abundance  $n(\ell) \sim P(\ell)\mu^\ell$ , where  $P(\ell)$  is a polynomial and  $\mu$  is the connective constant on hypercubic lattice which is  $\mu \sim 8.84$  for 5-dimensional hypercubic lattice [49]. Thus the critical temperature below which the loop error is self correcting is given by

$$e^{-2\beta_c} \mu \geq 1 \Rightarrow T_c \geq \frac{2}{\log \mu k_B} \sim 0.92/k_B, \quad (70)$$

where  $\beta_c = 1/T_c$ ,  $k_B$  is the Boltzmann constant, and the energy is measured in the unit such that the smallest loop of four lattice edges has energy  $2 \times 4 = 8$ . The above analysis is for one type of loop excitation, but it applies to three types of loop excitations, where the probability combining the Boltzmann factor and the entropy is raised to the third power. More precisely, this means that below the critical temperature, there exists  $L' > \xi L$  such that the critical probability for the logical membrane operator for loop excitations satisfy

$$\begin{aligned} P_{\text{crit}} &< \sum_{\ell > L'} n(\ell) e^{-2\beta\ell} \\ &< \sum_{\ell > L'} e^{-(2\beta - \log \mu)\ell} \text{Poly}(\ell) < \text{Poly}(L) \sum_{\ell > L'} e^{-(2\beta - \log \mu)\ell} \\ &< \text{Poly}(L) e^{-(2\beta - \log \mu)\xi L} \frac{1}{1 - e^{-(2\beta - \log \mu)}} \end{aligned} \quad (71)$$

is exponentially small in the system size, where we use  $\text{Poly}(\ell) < \text{Poly}(L)$ .

We note that the above analysis also equivalently establishes a probabilistic local cellular-automaton decoder for the loop excitation errors in the context of active error correction, where the local decoder simulates the local system-bath interaction. In particular, Eq. (68) and (69), along with the 1/2-probability plaquette flipping for the configurations with two violated edges, define a local update rule of for the cellular-automaton decoder at each syndrome measurement cycle. Note that either the measurement or the recovery operation has certain error probability. An error threshold for this decoder can be obtained via the effective critical temperature:  $p_c \sim e^{-8\beta_c}$  [1]. Due to the local nature of the decoder, there is no non-local classical communication required in the decoding process, which hence does not lead to a classical communication/computation overhead as the system scales, in contrast to the case of the usual non-local decoders.

*b. Errors inducing membrane excitations* Now let us analyze the membrane excitation error in a similar manner. The smallest membrane excitation corresponds to violating the flux term on a cube  $s_3$ , which is a  $5-3 = 2$  dimensional membrane on the dual lattice. Let us consider the flux for  $a$ . Then the Gauss law term for  $b, c$  will have energy cost 1 for the edge  $s_1, s'_1$  such that

$\int \tilde{s}_3 \cup \tilde{s}_1 \cup \tilde{s}'_1 = 1$ . The cube  $s_3$  corresponds to one surface  $s_2$  such that  $\int \tilde{s}_3 \cup \tilde{s}_2 = 1$  on 5-dimensional hypercubic lattice, and the edges  $s_1, s'_1$  can be two ordered consecutive edges on the boundary of the surface  $s_2$ . Thus there are four Gauss law terms contribute to energy cost  $1 \times 4 = 4$ , with a total energy  $4 \times 1 + 2 \times 1 = 6$ , where the second term is from the flux term on the cube. The smallest membrane excitation created by a single Pauli  $X_f^i$ , say  $i = 1$ , consists of 6 cubes from the  $2 \times (5-2) = 6$  directions perpendicular to the face  $f$  in both positive and negative directions. Let us consider the following transition probabilities:

- Creation or survival of a small membrane excitation, i.e. fluxes on 6 cubes:

$$\frac{P(0 \rightarrow 6)}{P(0 \rightarrow 0)} = \frac{P(6 \rightarrow 6)}{P(6 \rightarrow 0)} = e^{-36\beta}. \quad (72)$$

- Deforming the membrane excitation with fluxes on  $1 \rightarrow 5$  cubes or  $5 \rightarrow 1$  cubes:

$$\frac{P(1 \rightarrow 5)}{P(1 \rightarrow 1)} = \frac{P(5 \rightarrow 5)}{P(5 \rightarrow 1)} = e^{-24\beta}. \quad (73)$$

- Deforming the membrane excitation with fluxes on  $2 \rightarrow 4$  cubes or  $4 \rightarrow 2$  cubes:

$$\frac{P(2 \rightarrow 4)}{P(2 \rightarrow 2)} = \frac{P(4 \rightarrow 4)}{P(4 \rightarrow 2)} = e^{-12\beta}. \quad (74)$$

- Deforming the membrane excitation with fluxes on  $3 \rightarrow 3$  cubes: one can set the cube flipping probability at unit time to be 1/2 which connects different configurations and ensures ergodicity.

To estimate the critical temperature, we will need to balance the Boltzmann suppression  $e^{-6\beta A}$  for membrane excitations of area  $A$  and the entropy of the membrane. The latter can be estimated from self-avoiding random surfaces on 5-dimensional hypercubic dual lattice, which is discussed in e.g. Ref. [83]. The abundance again grows as  $e^{A/\tau_0}$  for some constant  $\tau_0$ , thus the critical temperature is  $T'_c \geq 6\tau_0/k_B$ . A probabilistic cellular automaton decoder is also present for the membrane excitation errors, similar to the one discussed above for the loop excitation errors. Below the critical temperature, there exists  $A' > (\xi L)^2$  such that the critical probability for the logical volume operator for membrane excitations satisfy

$$\begin{aligned} P_{\text{crit}} &< \sum_{A > A'} n(A) e^{-6\beta A} \\ &< \sum_{A > A'} e^{-(6\beta - 1/\tau_0)A} \text{Poly}(A) < \text{Poly}(L) \sum_{A > A'} e^{-(6\beta - 1/\tau_0)\ell} \\ &< \text{Poly}(L) e^{-(6\beta - 1/\tau_0)(\xi L)^2} \frac{1}{1 - e^{-(6\beta - 1/\tau_0)}} \end{aligned} \quad (75)$$

is exponentially small in the system size, where we use  $\text{Poly}(A) < \text{Poly}(L)$ .

Combining the results from the loop and membrane excitations, for temperature below  $\min(T_c, T'_c)$ , using the equations (67), (71) and (75) we complete the proof that the quantum memory is self-correcting.

Note that the above transition probabilities (Eq. (72) to (74) and the additional 1/2-probability transition rule) also equivalently establish a probabilistic local cellular automaton decoder for the membrane excitation errors.

### C. Readout of the memory and decoding the logical information

We have analyzed the error suppression during the process of the quantum computation, while there always exist residual errors that are never completely corrected. In the end of the quantum computation, we need to measure the encoded logical qubits in a certain logical basis. This can be done by performing a readout of all the qubits in a certain basis and then measure the corresponding logical operators. A convenient choice for this code is to measure all the qubits in the  $Z$  basis, which enables the measurement of electric Wilson membrane operators which have a product form  $\prod Z_f^i$ . Now in order to extract the encoded logical information, we assume that a reliable classical computer can help with decoding the measured classical data. Note that the measured data will contain errors originated from e.g. the thermal and readout noise. The errors in the Pauli-Z measurement can be detected via the error syndromes corresponding to the Gauss term, i.e., loop excitations. We then apply the probabilistic local cellular automaton decoder (for the loop excitation errors) presented above to clean up the loop excitations. Since the classical computer is reliable, this recovery process can be executed perfectly. One can then perform a readout on the Wilson membrane operators  $\prod Z_f^i$ . Note that a logical error can occur if the above recovery process creates a homologically non-trivial worldsheet of the loop excitations. Such a logical error can be exponentially suppressed with the system size  $L$  when the bath temperature is below the critical temperature  $\min(T_c, T'_c)$  and the readout error is below the error threshold of this decoder  $p_c \sim e^{-8\beta_c}$ .

### D. Generalization: general cubic theory without particles

Let us generalize the argument to general cubic theory without particles, with  $m, n, D$  satisfying (34). The theory consists of electric excitations of  $(m-1), (n-1), (D-m-n-1) \geq 1$  dimensions and magnetic excitations of  $(D-m-2), (D-n-2), (m+n-2) \geq 1$  dimensions. The thermal stability depends on the balance between the Boltzmann suppression and the entropy.

- The energy cost for the  $k$ -dimensional electric excitations is  $2\epsilon_0 V_k$  where the Hamiltonian has coefficient  $\epsilon_0$  and  $V_k$  is the volume of the excita-

tions in terms of the lattice spacing. The energy cost for the  $k'$ -dimensional magnetic excitations is  $(\epsilon_0 + 2\epsilon_0)V_{k'} = 3\epsilon_0 V_{k'}$ . The energy gap is thus bounded below by  $2\epsilon_0 V_k$  for  $k$ -dimensional excitation.

- The multiplicity of  $k$ -dimensional excitation of volume  $V_k$  for  $k \geq 1$  can be estimated as follows, following [1]. The first step of the random “submanifold-walk” on hypercubic lattice chooses  $k$  distinct directions out of  $2D$  directions (including the orientation), and the next step on chooses a boundary of this  $k$ -simplex to attach with another  $k$ -simplex, thus one first make a choice out of  $2k$  (including the orientation), and then one attaches to the original  $k$ -simplex with a new one by combining the boundary with one orthogonal direction not overlap with the original  $k$ -simplex, which is a choice of  $2D - k$ . Thus the multiplicity of  $V_k$  steps is bounded above by

$$n(V_k) \leq 2D(2k(2D - k))^{V_k}. \quad (76)$$

To suppress large excitations, it is sufficient to require the temperature to be lower than  $1/(\beta k_B)$  where

$$e^{-\beta 2\epsilon_0 V_k} 2D(2k(2D - k))^{V_k} \sim 1. \quad (77)$$

In other words, this gives an estimation of the critical temperature below which there is no large  $k$ -dimensional excitations

$$T_c(k) \sim \frac{2\epsilon_0}{\log(2k(2D - k))k_B}. \quad (78)$$

The critical temperature for all excitations is then

$$T_c \sim \min_{k \in S_{m,n}} T_c(k), \\ S_{m,n} := \{(l-1), (m-1), (n-1), \\ (D-l-2), (D-m-2), (D-n-2)\}. \quad (79)$$

We remark that if  $k \rightarrow 0$ , i.e. particle excitations, the estimation gives  $T_c(k) \rightarrow 0$  and  $T_c \rightarrow 0$ , which is consistent with thermal instability for topological orders with particles.

## VIII. DISCUSSION AND OUTLOOK

In this work we have constructed a family of infinite many candidate non-Abelian self-correcting quantum memories in spacetime dimension  $D \geq 5+1$ , which is the dimension that the non-Abelian self-correcting memories can occur. These models also give rise to the first set of non-Abelian topological orders which are stable at finite temperature. The models can be described by three  $\mathbb{Z}_2$  higher-form gauge fields with cubic topological interaction among them. In these models, the electric excitations obey Abelian fusion rules, while the magnetic



excitations obey non-Abelian fusion rules. We discuss the properties of the models using field theory and non-Pauli stabilizer lattice Hamiltonian models. We rigorously prove the self-correcting properties with a lower bound of the memory time and the thermal stability, and devise a probabilistic local cellular-automaton decoder for these codes.

There are several future directions. One can develop a deterministic cellular-automaton decoder using non-equilibrium dynamics in analogy to Toom's rule or sweep decoder [84], which is more efficient in cleaning up the errors than the current probabilistic decoder. Besides the study of the memory storage, the non-Abelian nature of this code can potentially allow us to perform non-Clifford and universal logical gate set in a self-correcting memory in five spatial dimensions, which would be lower dimensional than the current universal computation scheme with self-correcting memory based on a (6+1)D color code [5]. Also, the distance scaling of the non-Abelian self-correcting memory  $d = O(N^{\frac{2}{5}})$  is better than that of the (6+1)D color code  $d = O(N^{\frac{1}{3}})$  for total number of qubits equal  $N$ . Such fault-tolerant computing scheme will be highly desirable since it does not need non-local classical communication and there is no classical decoding overhead during the quantum computation process except the final readout stage when quantum operation already stops.

Finally, in our discussion we have focused on topological orders with fully-mobile excitations. It would be interesting to explore more general fractonic non-Abelian quantum memories in even lower spatial dimensions, where the code space can have exponentially many logical qubits in the system size.

## ACKNOWLEDGEMENTS

We thank Yu-An Chen and Nathanan Tantivasadakarn for discussions. We thank Maissam Barkeshli, Xie Chen, Meng Cheng, Shu-Heng Shao and Dominic J. Williamson for comments on a draft. P.-S.H. was supported by Simons Collaboration of Global Categorical Symmetry, Department of Mathematics King's College London, and also supported in part by grant NSF PHY-2309135 to the Kavli Institute for Theoretical Physics (KITP). R.K. is supported by the JQI postdoctoral fellowship at the University of Maryland, the U.S. Department of Energy and the Sivian Fund. G.Z. is supported by the U.S. Department of Energy, Office of Science, National Quantum Information Science Research Centers, Co-design Center for Quantum Advantage (C2QA) under contract number DE-SC0012704. P.-S.H. thanks Kavli Institute for Theoretical Physics for hosting the program "Correlated Gapless Quantum Matter" in 2024, during which part of the work is completed. We thank Peter Shor for posing the question about non-Abelian topological orders on Twitter, which partially inspired this work.

## Appendix A: Obstruction to Non-Abelian Fusion

Let us generalize the argument in [33–35] that rule out TQFTs with non-Abelian loop excitations in the absence of particles.

Consider TQFTs without  $(n-1)$ -dimensional excitations, where we take  $n \geq 2$ . Suppose there are  $n$ -dimensional simple excitations  $p_i$  with non-Abelian fusion rules on  $S^1 \times S^{n-1}$ :

$$p_1 \times p_2 = \sum_{i=3,4,\dots} p_i, \quad (\text{A1})$$

where  $p_i$  can be the same when the multiplicity is greater than one. We can shrink the  $S^1$  to a point, then the  $n$ -dimensional excitations become  $(n-1)$ -dimensional excitations on  $S^{n-1}$ . For simple  $n$ -dimensional excitations, the reduction on a circle gives an excitation that contains at most one copy of identity. Since there is no nontrivial  $(n-1)$ -dimensional excitations, this gives only the identity. The fusion rule (A1) becomes

$$1 \times 1 = \sum_{i=3,4,\dots} 1. \quad (\text{A2})$$

Thus we have a contradiction unless there is only one term on the right hand side. In other words, the fusion of the  $n$ -dimensional excitations is Abelian.

## Appendix B: Review of Cup Product on Triangulated and Hypercubic Lattices

Let us review cup product for  $\mathbb{Z}_2$  valued cochains on triangulated lattice and hypercubic lattice. For more details, see e.g. [42, 56–59].

A  $\mathbb{Z}_2$ -valued  $m$ -cochain  $\alpha_m$  is a map from  $m$ -simplices on the lattice to  $0, 1 \pmod 2$ . The cup product of  $m$ -cochain  $\alpha_m$  and  $n$ -cochain  $\beta_n$  is an  $(m+n)$ -cochain  $\alpha_m \cup \beta_n$  defined as follows:

- For triangulated lattice, denote  $k$ -simplices by the vertices  $s_k = (0, 1, 2, 3, \dots, k)$ , the cup product takes the following value on  $(m+n)$ -simplices:

$$\begin{aligned} \alpha_m \cup \beta_n(0, 1, 2, \dots, m+n) \\ = \alpha_m(0, 1, \dots, m)\beta_n(m, m+1, \dots, m+n). \end{aligned} \quad (\text{B1})$$

We note that there is a common vertex  $m$ .

- For hypercubic lattice, the cup product  $\alpha_m \cup \beta_n$  on  $(m+n)$ -dimensional hypercube  $s_{m+n}$  that span the coordinates  $(x^1, x^2, \dots, x^{m+n}) \in [0, 1]^{m+n}$  is given by

$$\begin{aligned} \alpha_m \cup \beta_n(s_{m+n}) \\ = \sum_I \alpha_m([0, 1]^I) \beta_n\left((x^I = 1, x^{\bar{I}} = 0) + [0, 1]^{\bar{I}}\right) \end{aligned} \quad (\text{B2})$$



where the summation is over the different sets  $I$  of  $m$  coordinates out of the  $(m+n)$  coordinates  $x^1, \dots, x^{m+n}$ ,  $\bar{I}$  denotes the remaining  $n$  coordinates. In each term in the sum,  $\alpha_m, \beta_n$  are evaluated on an  $m$ -dimensional hypercube and an  $n$ -dimensional hypercube, where the two hypercubes intersect at a point ( $x^I = 1, x^{\bar{I}} = 0$ ):

- $[0, 1]^I$  is the  $m$ -dimensional unit hypercube starting from ( $x^I = 0, x^{\bar{I}} = 0$ ) and ending at ( $x^I = 1, x^{\bar{I}} = 0$ ), i.e.  $[0, 1]^I = \{0 \leq x^i \leq 1, x^j = 0 : i \in I, j \in \bar{I}\}$ .
- $(x^I = 1, x^{\bar{I}} = 0) + [0, 1]^{\bar{I}}$  is the  $n$ -dimensional hypercube in the  $\bar{I}$  directions starting from ( $x^I = 1, x^{\bar{I}} = 0$ ) and ending at ( $x^I = 1, x^{\bar{I}} = 1$ ), i.e.  $(x^I = 1, x^{\bar{I}} = 0) + [0, 1]^{\bar{I}} = \{x^i = 1, 0 \leq x^j \leq 1 : i \in I, j \in \bar{I}\}$ .

### Appendix C: Logical CZ, S, Hadamard Gates in 4D Loop Toric Code

We will discuss the logical gates in the loop toric code model in (4+1)D, which is an example of self-correcting quantum memory at finite temperature (e.g. [1, 2]). The Hamiltonian is a stabilizer model:

$$H = H_{\text{Gauss}} + H_{\text{Flux}} = - \sum_e \prod_{f \in \partial e} X_f - \sum_c \prod_{f \in \partial c} Z_f, \quad (\text{C1})$$

where the  $\mathbb{Z}_2$  2-form gauge field is  $a_f = (1 - Z_f)/2$ . The ground states on  $M_4$  4-manifold is given by  $q$  qubits with  $H^2(M_4, \mathbb{Z}_2) = \mathbb{Z}_2^q$ .

The loop toric code has loop excitations labelled by the electric and magnetic charges  $(q_e, q_m)$  with  $q_e, q_m = 0, 1$ , i.e. pure electric loop (1, 0), pure magnetic loop (0, 1) and dyon loop (1, 1), corresponding to violation of the Gauss law terms along the loop, flux terms along the loop and both types of Hamiltonian terms along the loop.

#### 1. Hadamard gate

The model on hypercubic lattice has electromagnetic duality spin rotation symmetry that exchanges  $X \leftrightarrow Z$ , and swaps the lattice with the dual lattice. To see this, we note that the Gauss law term on edge in the  $x$  direction has product over  $X_f$  spanning  $x$  direction and one

of the remaining  $4 - 1 = 3$  directions, and taking into account the orientation the product is over  $3 \times 2 = 6$   $X_f$ . Similarly, each cube  $c$  spanning  $x, y, z$  directions has faces in  $xy, yz, zx$  directions, with orientations there are in total  $3 \times 2 = 6$   $Z_f$  in the product of each flux term.

On the loop excitations the symmetry acts as  $S : (q_e, q_m) \leftrightarrow (q_m, q_e)$ , where we note  $-q_m = q_m \pmod{2}$ , as well as  $T : (q_e, q_m) \rightarrow (q_e + q_m, q_m)$  [42, 85]. The  $S$  symmetry acts as Hadamard gate.

#### 2. CZ and S gates

The  $T : (q_e, q_m) \rightarrow (q_e + q_m, q_m)$  symmetry is generated by the gauged SPT defect decorated with  $H^4(B^2\mathbb{Z}_2, U(1)) = \mathbb{Z}_4$ : [42]

$$U(M_4) = i^{\int \mathcal{P}(a)}. \quad (\text{C2})$$

The gauged SPT phase on the domain wall is the semion Walker Wang model. The operator acting the ground states labelled by holonomy  $\{n_i = 0, 1\}$  for  $i = 1, 2, \dots, q$  according to the intersection form  $M_{ij}$  on  $H^2(M_4)$ :

$$U(M_4)|\{n_i\}\rangle = i^{\sum_j M_{jj}n_j^2} (-1)^{\sum_{i < j} M_{ij}n_i n_j} |\{n_i\}\rangle. \quad (\text{C3})$$

Consider the following cases:

- $M_4 = T_{x,y,z,w}^4$ , with  $q = 6$ . The operator realizes the logical gate

$$U(T^4) = \text{CZ}_{xy,zw} \text{CZ}_{xz,yw} \text{CZ}_{yz,xw}, \quad (\text{C4})$$

where  $xy$  is the 2-cycle spanning  $x, y$  directions, and similarly for  $zw, xz, yw, yz, xw$ .

In particular, this implies that  $U(T^4)X_{xy}U(T^4)^{-1} = X_{xy}Z_{zw}$ , where  $X, Z$  are the logical gates. Thus the symmetry permutes the magnetic loop excitation to the dyon loop excitation. This is the case considered in [42].

- $M_4 = \mathbb{C}\mathbb{P}^2$ , with  $q = 1$ . The operator realizes the logical gate

$$U(T^4) = S. \quad (\text{C5})$$

In other words, if the state has trivial holonomy on the 2-cycle, the operator acts trivially; if the state has nontrivial holonomy on the 2-cycle, the operator acts as  $i$ .

---

[1] E. Dennis, A. Kitaev, A. Landahl, and J. Preskill, *J. Math. Phys.* **43**, 4452 (2002), arXiv:quant-ph/0110143.  
[2] B. J. Brown, D. Loss, J. K. Pachos, C. N. Self, and J. R. Wootton, *Reviews of Modern Physics* **88**, 10.1103/revmodphys.88.045005 (2016).  
[3] H. Bombin, *Phys. Rev. X* **5**, 031043 (2015).

[4] R. Alicki, M. Horodecki, P. Horodecki, and R. Horodecki, *Open Systems & Information Dynamics* **17**, 1 (2010).  
[5] H. Bombin, R. W. Chhajlany, M. Horodecki, and M. A. Martin-Delgado, *New Journal of Physics* **15**, 055023 (2013).  
[6] N. Berthussen, J. Dreiling, C. Foltz, J. P. Gaebler, T. M.

- Gatterman, D. Gresh, N. Hewitt, M. Mills, S. A. Moses, B. Neyenhuis, P. Siegfried, and D. Hayes, *Experiments with the 4d surface code on a qccd quantum computer* (2024), [arXiv:2408.08865 \[quant-ph\]](#).
- [7] L. Guth and A. Lubotzky, *Journal of Mathematical Physics* **55**, 082202 (2014).
- [8] N. P. Breuckmann and V. Londe, *arXiv quant-ph* (2020), [2001.03568](#).
- [9] M. Freedman and M. B. Hastings, *arXiv:2012.02249* (2020).
- [10] S. Bravyi, A. W. Cross, J. M. Gambetta, D. Maslov, P. Rall, and T. J. Yoder, *Nature* **627**, 778 (2024).
- [11] N. P. Breuckmann, C. Vuillot, E. Campbell, A. Krishna, and B. M. Terhal, *Quantum Science and Technology* **2**, 035007 (2017).
- [12] M. Hastings, J. Haah, and R. O’Donnell, in *Proc. ACM STOC* (Association for Computing Machinery, New York, NY, USA, 2021) pp. 1276–1288.
- [13] P. Panteleev and G. Kalachev, *IEEE Trans. Inf. Theo.* **68**, 213 (2022).
- [14] N. P. Breuckmann and J. N. Eberhardt, *IEEE Trans. Inf. Theo.* **67**, 6653 (2021).
- [15] M. Hastings, *arXiv:2102.10030* (2021).
- [16] P. Panteleev and G. Kalachev, in *Proc. ACM STOC* (Association for Computing Machinery, New York, NY, USA, 2022) pp. 375–388.
- [17] A. Leverrier and G. Zemor, in *Proc. IEEE FOCS* (IEEE Computer Society, Los Alamitos, CA, USA, 2022) pp. 872–883.
- [18] T. Lin and M. Hsieh, *arXiv:2203.03581* (2022).
- [19] S. Gu, C. Pattison, and E. Tang, *arXiv:2206.06557* (2022).
- [20] I. Dinur, M. Hsieh, T. Lin, and T. Vidick, in *Proc. ACM STOC* (Association for Computing Machinery, New York, NY, USA, 2023) pp. 905–918.
- [21] A. Leverrier and G. Zémor, Efficient decoding up to a constant fraction of the code length for asymptotically good quantum codes, in *Proc. ACM SODA* (2023) pp. 1216–1244.
- [22] S. Gu, E. Tang, L. Caha, S. Choe, Z. He, and A. Kubica, *arXiv:2306.12470* (2023).
- [23] G. Zhu, S. Sikander, E. Portnoy, A. W. Cross, and B. J. Brown, *arXiv preprint arXiv:2310.16982* (2023).
- [24] M. H. Freedman, M. Larsen, and Z. H. Wang, *Communications in Mathematical Physics* **227**, 605 (2002).
- [25] M. A. Levin and X.-G. Wen, *Phys. Rev. B* **71**, 045110 (2005).
- [26] R. Koenig, G. Kuperberg, and B. W. Reichardt, *Annals of Physics* **325**, 2707 (2010).
- [27] A. Schotte, G. Zhu, L. Burgelman, and F. Verstraete, *Phys. Rev. X* **12**, 021012 (2022).
- [28] Z. K. Mineev, K. Najafi, S. Majumder, J. Wang, A. Stern, E.-A. Kim, C.-M. Jian, and G. Zhu, *arXiv preprint arXiv:2406.12820* (2024).
- [29] Z. Nussinov and G. Ortiz, *Physical Review B* **77**, 10.1103/physrevb.77.064302 (2008).
- [30] S. Bravyi and B. Terhal, *New Journal of Physics* **11**, 043029 (2009).
- [31] M. B. Hastings, *Phys. Rev. Lett.* **107**, 210501 (2011).
- [32] B. Yoshida, *Annals of Physics* **326**, 2566–2633 (2011).
- [33] T. Johnson-Freyd and M. Yu, *Bull. Austral. Math. Soc.* **104**, 434 (2021), [arXiv:2010.07950 \[math.QA\]](#).
- [34] T. Johnson-Freyd and M. Yu, *SciPost Phys.* **13**, 068 (2022), [arXiv:2104.04534 \[hep-th\]](#).
- [35] C. Cordova, P.-S. Hsin, and C. Zhang, *Anomalies of Non-Invertible Symmetries in (3+1)d* (2023), [arXiv:2308.11706 \[hep-th\]](#).
- [36] A. Kitaev, *Annals Phys.* **303**, 2 (2003).
- [37] M. Iqbal *et al.*, *Nature* **626**, 505 (2024), [arXiv:2305.03766 \[quant-ph\]](#).
- [38] E. T. Campbell, B. M. Terhal, and C. Vuillot, *Nature* **549**, 172 (2017).
- [39] G. Zhu, A. Lavasani, and M. Barkeshli, *Phys. Rev. Lett.* **125**, 050502 (2020).
- [40] G. Zhu, A. Lavasani, and M. Barkeshli, *Phys. Rev. B* **102**, 075105 (2020).
- [41] A. Lavasani, G. Zhu, and M. Barkeshli, *Quantum* **3**, 180 (2019).
- [42] X. Chen, A. Dua, P.-S. Hsin, C.-M. Jian, W. Shirley, and C. Xu, *Loops in 4+1d Topological Phases* (2021), [arXiv:2112.02137 \[cond-mat.str-el\]](#).
- [43] L. Kong and X.-G. Wen, *Braided fusion categories, gravitational anomalies, and the mathematical framework for topological orders in any dimensions* (2014), [arXiv:1405.5858 \[cond-mat.str-el\]](#).
- [44] L. Kong, X.-G. Wen, and H. Zheng, *Boundary-bulk relation for topological orders as the functor mapping higher categories to their centers* (2015), [arXiv:1502.01690 \[cond-mat.str-el\]](#).
- [45] L. Kong, X.-G. Wen, and H. Zheng, *Nuclear Physics B* **922**, 62–76 (2017).
- [46] T. Johnson-Freyd, *Communications in Mathematical Physics* **393**, 989–1033 (2022).
- [47] D. Gaiotto and T. Johnson-Freyd, *Condensations in higher categories* (2019), [arXiv:1905.09566 \[math.CT\]](#).
- [48] B. Yoshida, *Phys. Rev. B* **93**, 155131 (2016).
- [49] N. Madras and G. Slade, *The Self-Avoiding Walk*, Modern Birkhäuser Classics (Springer New York, 2012).
- [50] H. Bombin, R. W. Chhajlany, M. Horodecki, and M. A. Martin-Delgado, *New Journal of Physics* **15**, 055023 (2013).
- [51] X. Chen, Z.-C. Gu, Z.-X. Liu, and X.-G. Wen, *Phys. Rev. B* **87**, 155114 (2013), [arXiv:1106.4772 \[cond-mat.str-el\]](#).
- [52] M. D. F. de Wild Propitius, *Topological interactions in broken gauge theories*, Ph.D. thesis, Amsterdam U. (1995), [arXiv:hep-th/9511195](#).
- [53] B. Yoshida, *Phys. Rev. B* **93**, 155131 (2016), [arXiv:1508.03468 \[cond-mat.str-el\]](#).
- [54] L. Tsui and X.-G. Wen, *Phys. Rev. B* **101**, 035101 (2020), [arXiv:1908.02613 \[cond-mat.str-el\]](#).
- [55] Y.-A. Chen and P.-S. Hsin, *SciPost Phys.* **14**, 089 (2023), [arXiv:2110.14644 \[cond-mat.str-el\]](#).
- [56] J. Milnor, J. Stasheff, J. Stasheff, and P. University, *Characteristic Classes*, Annals of mathematics studies (Princeton University Press, 1974).
- [57] F. Benini, C. Córdova, and P.-S. Hsin, *JHEP* **03**, 118, [arXiv:1803.09336 \[hep-th\]](#).
- [58] L. Tsui and X.-G. Wen, *Phys. Rev. B* **101**, 035101 (2020).
- [59] Y.-A. Chen and S. Tata, *Higher cup products on hypercubic lattices: application to lattice models of topological phases* (2021), [arXiv:2106.05274 \[cond-mat.str-el\]](#).
- [60] M. Levin and Z.-C. Gu, *Phys. Rev. B* **86**, 115109 (2012).
- [61] L. Bhardwaj, D. Gaiotto, and A. Kapustin, *JHEP* **04**, 096, [arXiv:1605.01640 \[cond-mat.str-el\]](#).
- [62] W. Shirley, K. Slagle, and X. Chen, *SciPost Phys.* **6**, 041 (2019), [arXiv:1806.08679 \[cond-mat.str-el\]](#).
- [63] M. Barkeshli, Y.-A. Chen, P.-S. Hsin, and R. Kobayashi, *SciPost Phys.* **16**, 089 (2024), [arXiv:2211.11764 \[cond-](#)

- mat.str-el].
- [64] M. Barkeshli, P.-S. Hsin, and R. Kobayashi, *SciPost Phys.* **16**, 122 (2024), arXiv:2311.05674 [cond-mat.str-el].
- [65] M. Barkeshli, P. Bonderson, M. Cheng, and Z. Wang, *Phys. Rev. B* **100**, 115147 (2019), arXiv:1410.4540 [cond-mat.str-el].
- [66] J. C. Teo, T. L. Hughes, and E. Fradkin, *Annals of Physics* **360**, 349–445 (2015).
- [67] N. Tarantino, N. H. Lindner, and L. Fidkowski, *New Journal of Physics* **18**, 035006 (2016).
- [68] M. de Wild Propitius, *Physics Letters B* **410**, 188 (1997).
- [69] A. Coste, T. Gannon, and P. Ruelle, *Nucl. Phys. B* **581**, 679 (2000), arXiv:hep-th/0001158.
- [70] P.-S. Hsin and A. Turzillo, *JHEP* **09**, 022, arXiv:1904.11550 [cond-mat.str-el].
- [71] E. Witten, *J. Geom. Phys.* **22**, 103 (1997), arXiv:hep-th/9610234.
- [72] E. Witten, *JHEP* **12**, 012, arXiv:hep-th/9812012.
- [73] E. Witten, *Geometric Langlands From Six Dimensions* (2009), arXiv:0905.2720 [hep-th].
- [74] D. S. Freed and C. Teleman, *Commun. Math. Phys.* **326**, 459 (2014), arXiv:1212.1692 [hep-th].
- [75] C. Córdova, D. Costa, and P.-S. Hsin, To appear.
- [76] B. Yoshida, *Phys. Rev. B* **91**, 245131 (2015).
- [77] B. Yoshida, *Annals of Physics* **377**, 387 (2017).
- [78] M. Barkeshli, Y.-A. Chen, S.-J. Huang, R. Kobayashi, N. Tantivasadakarn, and G. Zhu, *SciPost Physics* **14**, 065 (2023).
- [79] P. Putrov, J. Wang, and S.-T. Yau, *Annals Phys.* **384**, 254 (2017), arXiv:1612.09298 [cond-mat.str-el].
- [80] A. Kubica, B. Yoshida, and F. Pastawski, *New J. Phys.* **17**, 083026 (2015), arXiv:1503.02065 [quant-ph].
- [81] H. Bombin and M. A. Martin-Delgado, *Phys. Rev. Lett.* **97**, 180501 (2006), arXiv:quant-ph/0605138.
- [82] J. J. Wallman and J. Emerson, *Phys. Rev. A* **94**, 052325 (2016), arXiv:1512.01098 [quant-ph].
- [83] B. Durhuus, J. Fröhlich, and T. Jonsson, *Nuclear Physics B* **225**, 185 (1983).
- [84] A. Dua, T. Jochym-O’Connor, and G. Zhu, *Quantum* **7**, 1122 (2023).
- [85] D. Gaiotto, A. Kapustin, N. Seiberg, and B. Willett, *JHEP* **02**, 172, arXiv:1412.5148 [hep-th].